

© 2020 by the Arizona Board of Regents on behalf of the University of Arizona. This is an Open Access article, distributed under the terms of the Creative Commons Attribution licence (<http://creativecommons.org/licenses/by/4.0/>), which permits unrestricted re-use, distribution, and reproduction in any medium, provided the original work is properly cited.

UPDATED CARIACO BASIN ^{14}C CALIBRATION DATASET FROM 0–60 CAL KYR BP

Konrad A Hughen^{1*}  • Timothy J Heaton²

¹Department of Marine Chemistry and Geochemistry, Woods Hole Oceanographic Institution, Woods Hole, MA 02543, USA

²School of Mathematics and Statistics, University of Sheffield, Sheffield S3 7RH, UK

ABSTRACT. We present new updates to the calendar and radiocarbon (^{14}C) chronologies for the Cariaco Basin, Venezuela. Calendar ages were generated by tuning abrupt climate shifts in Cariaco Basin sediments to those in speleothems from Hulu Cave. After the original Cariaco-Hulu calendar age model was published, Hulu Cave $\delta^{18}\text{O}$ records have been augmented with increased temporal resolution and a greater number of U/Th dates. These updated Hulu Cave records provide increased accuracy as well as precision in the final Cariaco calendar age model. The depth scale for the Ocean Drilling Program Site 1002D sediment core, the primary source of samples for ^{14}C dating, has been corrected to account for missing sediment from a core break, eliminating age-depth anomalies that afflicted the earlier calendar age models. Individual ^{14}C dates for the Cariaco Basin remain unchanged from previous papers, although detailed comparisons of the Cariaco calibration dataset to those from Hulu Cave and Lake Suigetsu suggest that the Cariaco marine reservoir age may have shifted systematically during the past. We describe these recent changes to the Cariaco datasets and provide the data in a comprehensive format that will facilitate use by the community.

KEYWORDS: calibration, climate, radiocarbon.

INTRODUCTION

Calibration of the ^{14}C timescale over its full length has advanced remarkably in recent decades. Several independent datasets now extend beyond ~50 cal kyr BP (Hughen et al. 2006; Bronk Ramsey et al. 2012; Cheng et al. 2018), displaying detailed shared structure and improving confidence in the general trends of the ^{14}C calibration curve, though differences still remain (Reimer et al. 2013, 2020 in this issue). Ocean Drilling Program (ODP) Site 1002, drilled in the Cariaco Basin off the coast of Venezuela, possesses high deposition rate sediments that are intermittently laminated, with annual varves during the last deglaciation and Holocene, but predominantly bioturbated sediments throughout the last Glacial period. Cariaco sediments contain detailed paleoclimate records showing abrupt millennial-scale climate shifts throughout the last Glacial period and beyond (Peterson et al. 2000). These millennial climate changes display abrupt shifts between quasi-stable states that occurred on timescales of decades or less (Hughen et al. 1996). Similar changes have been reported from other high-resolution archives, including Greenland ice cores (Johnsen et al. 1992) and speleothems from China (Wang et al. 2001), that possess calendar-age chronologies from layer-counting or U/Th dating. General circulation model (GCM) results show that reducing North Atlantic Meridional Overturning Circulation (AMOC), believed to have caused abrupt changes in high-latitude temperature, also result in “downstream” shifts in tropical Atlantic trade wind strength and monsoon rainfall over Asia (e.g., Rind et al. 1986; Manabe and Stouffer 1997). The Cariaco high-resolution paleoclimate records have therefore been “tuned” to the Greenland ice core (Meese et al. 1997) and Hulu Cave speleothem (Wang et al. 2001) records to provide calendar age models. Such paleoclimate tuning is based upon the identification of a set of tie-points, relating to shared abrupt palaeoclimatic events and assumed to be approximately contemporaneous, in both the Cariaco record and the Greenland/Hulu records from which chronological information can

*Corresponding author. Email: khughen@whoi.edu.

be transferred. The resulting Cariaco Basin ^{14}C calibration datasets (Hughen et al. 2004a, 2006) were used to help build the IntCal04, IntCal09 and IntCal13 calibration curves (Reimer et al. 2004, 2009, 2013; Hughen et al. 2004b).

Here, we present the results of tuning Cariaco Basin sediment reflectance data to revised, high-resolution Hulu Cave $\delta^{18}\text{O}$ records (Cheng et al. 2016) with updated U/Th chronologies (Cheng et al. 2018). This improvement in Hulu Cave resolution enables us to re-evaluate and improve our ties. Given these updated ties, we then use the same Gaussian Process methodology (Heaton et al. 2013) as used for the IntCal13 update, to propagate uncertainties in both the precise synchronicity of the selected ties and the Hulu U/Th dating through to the new Cariaco timescale. The updated Cariaco Basin ^{14}C calibration dataset is used to help build the IntCal20, SHCal20, and Marine20 ^{14}C calibration curves (Reimer et al. 2020 in this issue; Hogg et al. 2020 in this issue; Heaton et al. 2020b in this issue), and the data are provided here with replicate ^{14}C measurements reported as averages as well as individual dates.

Use of marine records in reconstructing atmospheric radiocarbon is complicated by the systematic ^{14}C depletion within surface-ocean environments known as a marine reservoir age (MRA), which may vary over time. To incorporate the Cariaco ^{14}C record into IntCal20, changes in the MRA for the Cariaco Basin through time were modeled as an additive spline and estimated during curve construction by comparison with all of the other constituent IntCal20 datasets (Heaton et al. 2020a in this issue). This additive approach enables the Cariaco Basin to contribute strength to the IntCal20 curve in the case where ^{14}C features are shared with other IntCal20 datasets; while reducing the impact of potentially spurious variation seen only in a single set. Further, it provides insight of potential independent interest into the magnitude and duration of MRA variability within the Cariaco Basin.

Notation: In this paper, both ^{14}C ages and calendar ages are reported relative to AD 1950 (= 0 BP, before present). To distinguish between them, ^{14}C ages are given in units “ ^{14}C yrs BP” while calendar/calibrated ages are given as “cal yr BP” or cal kyr BP (thousands of calibrated years before present). All quoted uncertainties on values, e.g. 420 ± 50 ^{14}C yrs, refer to the 1σ level.

Calendar Chronology

The Cariaco Basin ODP sediment record has no calendar age scale of its own, and rapid climate shifts in Cariaco and other, absolute-age, paleoclimate archives have been used to transfer calendar age models to the Cariaco record. Originally, the calendar-age chronology for the Site 1002 sediment record was constructed by aligning climate changes with the annual layer counted GISP2 Greenland ice core $\delta^{18}\text{O}$ record (Meese et al. 1997) (Figure 1), based on evidence for synchronous timing of rapid climate shifts within the timescale of one or two decades (Hughen et al. 1996, 2004c). Tie-points were based on rapid stadial-interstadial transitions (“warmings”) in Greenland, which have counterparts (reduced trade winds and increased precipitation) in the tropical North Atlantic region (Hughen et al. 2004a). In Hughen et al. (2006), the Cariaco record, including transitions both into and out of millennial events, was tuned to analogous hydrological changes in U/Th-dated speleothem $\delta^{18}\text{O}$ records from Hulu Cave (Wang et al. 2001). The Hulu Cave $\delta^{18}\text{O}$ records possessed relatively low temporal resolution, and there was some uncertainty in identifying precisely analogous signals in the two records, especially in the late Glacial period ~15–25

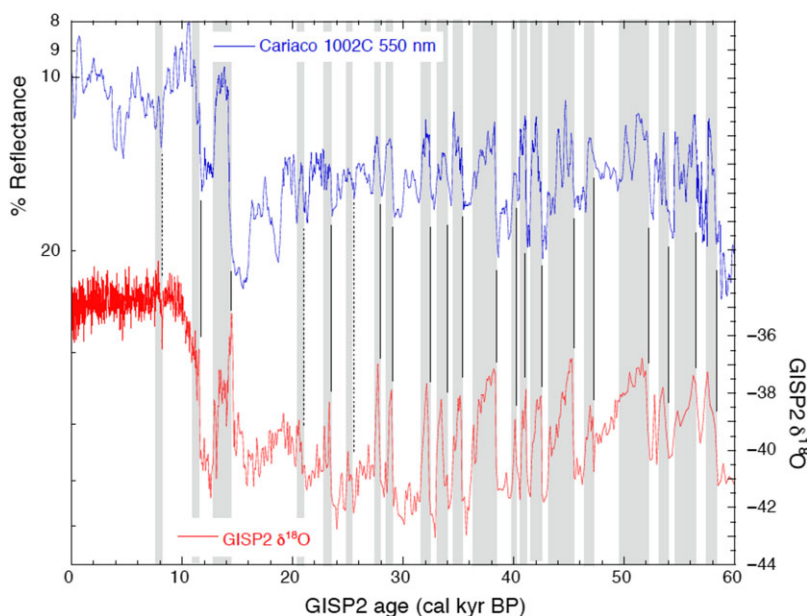


Figure 1 Comparison of paleoclimate records between the Cariaco Basin and Greenland ice cores: (upper) 550 nm reflectance from Cariaco sediments, showing periods of greater windiness (down) and greater rainfall (up). (lower) Oxygen isotopes from the GISP2 ice core, showing periods of increased cooling (down) and warmth (up). These tie points were used in creating the calendar age for the Cariaco Basin ^{14}C calibration dataset used in IntCal04. Figure adapted from Hughen et al. 2004a, supplementary documentation.

cal kyr BP (Hughen et al. 2006). The Hulu Cave speleothem records have since been updated with higher temporal resolution $\delta^{18}\text{O}$ measurements (Cheng et al. 2016) and a denser sequence of U/Th dates (Cheng et al. 2018), and the revised records show even stronger agreement with Cariaco Basin paleoclimate (Figure 2).

Sediment Depth Scale

The depth scale previously used for Cariaco Basin paleoclimate and ^{14}C records used in IntCal was based on ODP Site 1002 Hole D, from which the majority of samples for ^{14}C dating were obtained. A core-break occurred in Hole D near 14 mbsf, which was bridged using continuous sediments from adjacent Hole E (Hughen et al. 2004a). For consistency with sample identifications at ODP sediment core repositories, the Hole D depth scale was maintained, despite creating an anomaly in the age-depth curve around 14 mbsf (30–32 cal kyr BP) (Figure 3). Here, we have revised the depth scale by restoring 56 cm of missing sediment to the Hole D depth scale between 14.2 and 14.76 mbsf. Both original and adjusted depth scales are reported in Table 1.

Tie-Points

In this study, the tie points used to align the Cariaco Basin and Hulu Cave paleoclimate records were selected primarily at the rapid transitions between the tropical analogs of “stadial” and “interstadial” millennial climate events (i.e., “warmings” at high latitudes and increased precipitation in the tropics) (Figure 2). These are generally the same tie points used in Hughen et al. (2006), except that most of the less-rapid transitions between “interstadial”

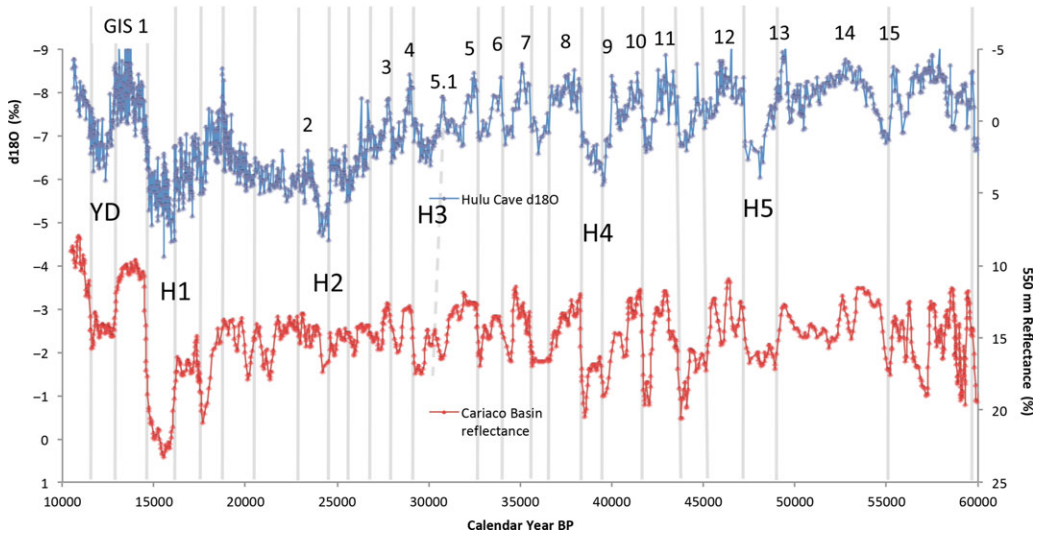


Figure 2 Comparison of paleoclimate records between the Cariaco Basin and Hulu Cave: (upper) Oxygen isotopes measured on calcite from Hulu Cave speleothems, showing wetter (up) and drier (down) conditions. (lower) 550 nm reflectance from Cariaco sediments, showing periods of greater windiness (down) and greater rainfall (up). These tie points are a subset of those used previously for the Cariaco Basin ^{14}C calibration dataset used in IntCal09 and IntCal13 and are used to create the calendar age for the current dataset.

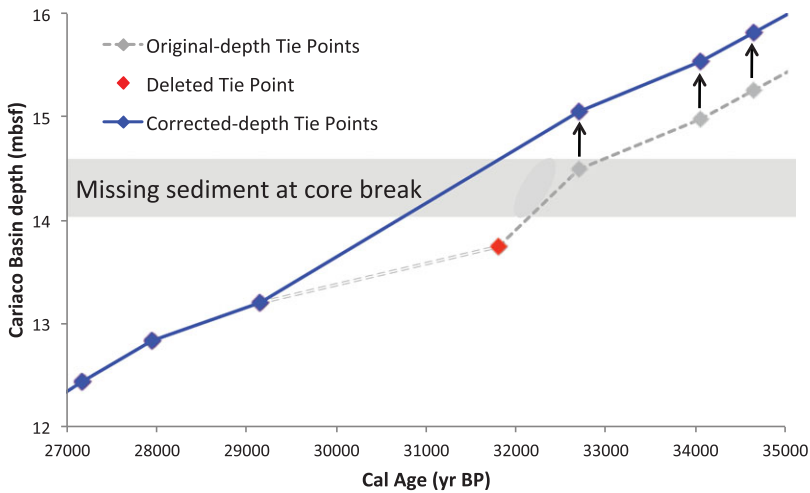


Figure 3 Close-up view of Cariaco-Hulu calendar age plotted versus Cariaco Basin sediment depth. 56 cm of sediment missing from a core-break below 14 mbsf have been restored to the original depth scale (gray), and the revised age-depth model (blue) showed an anomalous tie point around 32 cal kyr BP (red). This tie-point has been removed from the current age model.

and “stadial” events (i.e., high-latitude “coolings” or tropical “dryings”) have been eliminated due to the lower precision of the matches. We note that during the later Glacial period, from ~15–25 cal kyr BP, the tie points are less distinct, with greater variability in the Cariaco record than in Hulu. The remaining individual tie points were evaluated to identify anomalous

changes in sedimentation rate resulting from the revised depth scale. All identified tie-points were assumed to represent approximately synchronous events in the Hulu Cave and Cariaco Basin records, with an uncertainty in this contemporaneity of ± 100 cal yrs (1σ) for each tie incorporated into chronology construction.

One tie point, related to a relatively minor climate event correlated with Greenland Interstadial (GIS) 5.1 immediately preceding Heinrich Event (HE) 3 (Rasmussen et al. 2014) (Figure 2), created a sharp change in sedimentation rate at 30–32 cal kyr BP (Figure 3) and likely contributed to anomalously old calendar ages within this section in the Cariaco record and IntCal13 (Reimer et al. 2013). This spurious link has therefore been removed, eliminating the anomalous sedimentation rates and resulting in a smoother age-depth curve overall (Figure 4). The tie points were used as input into a Gaussian process model (Heaton et al. 2013) to create a continuous calendar age-depth model for the Cariaco Basin with associated age uncertainty estimates that propagate both our uncertainty in the Hulu timescale and the precise contemporaneity of the chosen ties.

^{14}C Chronology

The same ^{14}C data set used previously to help constrain ^{14}C calibration in IntCal09 and IntCal13 (Reimer et al. 2009, 2013) is plotted here versus the updated Cariaco Basin calendar chronology (Figure 5). In this plot, we have adjusted the Cariaco ^{14}C data sets based on a constant marine reservoir age (MRA) of 420 ± 50 ^{14}C yrs (Hughen et al. 2000). In addition to ^{14}C age, the absolute concentration of ^{14}C ($\Delta^{14}\text{C}$), corrected for isotopic fractionation and calendar age and reported relative to 1890 atmospheric values (Stuiver and Polach 1977), is plotted to amplify potential variability through time. The Cariaco data are plotted together with Hulu Cave (Cheng et al. 2018) and Lake Suigetsu (Bronk Ramsey et al. 2012) ^{14}C calibration data for comparison. The Hulu data set has been corrected for dead carbon fraction (DCF) under an assumption of a constant DCF of 450 ± 70 ^{14}C yrs to enable comparison.

All three datasets reveal close agreement, including prominent structures previously reported for the Glacial and Deglacial periods (e.g., Hughen et al. 2006; Bronk Ramsey et al. 2012; Cheng et al. 2018). These include the Laschamps geomagnetic minimum and period of rapid ^{14}C production from ~ 42 – 41 cal kyr BP, large oscillations from 40–30 cal kyr BP also attributed to geomagnetic variability (Laj et al. 2002; Hughen et al. 2004a), and a gradual overall decline after ~ 25 cal kyr BP due to increasing geomagnetic field strength and the end of Glacial climate conditions (Figure 5). The Lake Suigetsu data show a relatively higher degree of scatter than the other two records, and for clarity we show the Cariaco and Hulu data sets alone (Figure 6), although each plot is replicated including the Suigetsu data in the Supplementary Information (Figures S1–S7).

Marine Reservoir Age

Comparing the newly updated Cariaco Basin ^{14}C dataset to Hulu Cave ^{14}C in Figures 5 and 6, both plotted under the assumption of a constant level of MRA/DCF ^{14}C depletion, does however reveal several periods where apparent offsets exist, mostly consisting of younger ^{14}C ages (higher $\Delta^{14}\text{C}$ values) for the Cariaco Basin data. These are most evident around 18, 23, and 30 cal kyr BP. Potential explanatory factors for these periodic offsets include periodic misalignment of the Cariaco tuning; uncertainties in the calendar age chronologies which are not indicated in Figure 5 but are incorporated in construction of the IntCal20

Table 1 ^{14}C and calendar age data for the Cariaco Basin Site 1002D/E marine-derived ^{14}C calibration record. Lab identification and species information are provided for each ^{14}C date. All errors are 1 sigma. Dates obtained by averaging two or three replicate measurements are indicated on right. Data points removed due to anomalous values (compared to means and uncertainties taken from replicates or immediately adjacent bracketing samples) are also indicated on right with an "X"; (a) indicates samples from core breaks, (b) small samples deviating by >4 sigma, (c) samples from poorly performing wheel deviating by >4 sigma, (d) non-suspect samples deviating by >4 sigma. CAMS-LLNL refers to the Center for AMS at Lawrence Livermore National Laboratory.

ODP Hole	Section	Upper depth	Lower depth	Composite depth (mbsf)	Adjusted depth (mbsf)	AMS lab ID#	Species	CB_Hulu calendar age (yr BP)	Cal age \pm
1002D	1 H 1	5	7.5	0.063	0.06	NSRL-13105	bulloides		
1002D	1 H 1	40	42.5	0.413	0.41	NSRL-13106	bulloides		
1002D	1 H 1	50	52.5	0.513	0.51	CAMS-52110	bulloides		
1002D	1 H 1	55	57.5	0.563	0.56	NSRL-13107	bulloides		
1002D	1 H 1	100	102.5	1.013	1.01	CAMS-52111	bulloides		
1002D	1 H 2	0	2.5	1.513	1.51	CAMS-52112	bulloides		
1002D	1 H 2	50	52.5	2.013	2.01	CAMS-52113	bulloides		
1002D	1 H 2	100	102.5	2.513	2.51	CAMS-52114	bulloides		
1002D	1 H 3	0	2.5	3.013	3.01	CAMS-52115	bulloides		
1002D	1 H 3	25	27.5	3.263	3.26	NSRL-13048	bulloides		
1002D	1 H 3	50	52.5	3.513	3.51	CAMS-52116	bulloides		
1002D	1 H 3	75	77.5	3.763	3.76	NSRL-13049	bulloides		
1002D	1 H 4	0	2.5	4.013	4.01	CAMS-52117	bulloides		
1002D	1 H 4	25	27.5	4.263	4.26	NSRL-13050	bulloides		
1002D	1 H 4	45	47.5	4.463	4.46	CAMS-52118	bulloides		
1002D	2 H 1	0	2.5	4.713	4.71	NSRL-13051	ruber		
1002D	2 H 1	5	7.5	4.763	4.76	NSRL-13960	ruber		
1002D	2 H 1	10	12.5	4.813	4.81	NSRL-12273	bulloides		
1002D	2 H 1	10	12.5	4.813	4.81	NSRL-13961	ruber		
1002D	2 H 1	15	17.5	4.863	4.86	NSRL-13962	ruber		
1002D	2 H 1	20	22.5	4.913	4.91	NSRL-13052	bulloides		
1002D	2 H 1	20	22.5	4.913	4.91	NSRL-13963	ruber		
1002D	2 H 1	25	27.5	4.963	4.96	NSRL-13964	ruber		
1002D	2 H 1	30	32.5	5.013	5.01	CAMS-52119	bulloides	13563	137
1002D	2 H 1	30	32.5	5.013	5.01	CAMS-53659	ruber	13563	137
1002D	2 H 1	35	37.5	5.063	5.06	NSRL-13965	ruber	13693	139
1002D	2 H 1	40	42.5	5.113	5.11	NSRL-13053	bulloides	13822	138
1002D	2 H 1	40	42.5	5.113	5.11	NSRL-13966	ruber	13822	138
1002D	2 H 1	45	47.5	5.163	5.16	NSRL-13967	ruber	13948	136
1002D	2 H 1	50	52.5	5.213	5.21	NSRL-13054	bulloides	14072	132
1002D	2 H 1	50	52.5	5.213	5.21	NSRL-13968	ruber	14072	132
1002D	2 H 1	55	57.5	5.263	5.26	NSRL-13969	ruber	14193	126
1002D	2 H 1	60	62.5	5.313	5.31	NSRL-12274	bulloides	14312	120
1002D	2 H 1	60	62.5	5.313	5.31	NSRL-13970	ruber	14312	120
1002D	2 H 1	65	67.5	5.363	5.36	NSRL-13971	ruber	14428	114
1002D	2 H 1	70	72.5	5.413	5.41	NSRL-13055	bulloides	14541	110
1002D	2 H 1	70	72.5	5.413	5.41	NSRL-13972	ruber	14541	110
1002D	2 H 1	75	77.5	5.463	5.46	UCIAMS-16532	mixed	14652	108
1002D	2 H 1	75	77.5	5.463	5.46	CAMS-59349	ruber	14652	108
1002D	2 H 1	80	82.5	5.513	5.51	CAMS-52120	bulloides	14759	110
1002D	2 H 1	80	82.5	5.513	5.51	CAMS-53660	ruber	14759	110
1002D	2 H 1	85	87.5	5.563	5.56	UCIAMS-17584	bulloides	14863	115
1002D	2 H 1	85	87.5	5.563	5.56	CAMS-59350	ruber	14863	115
1002D	2 H 1	90	92.5	5.613	5.61	CAMS-59351	ruber	14964	121
1002D	2 H 1	95	97.5	5.663	5.66	UCIAMS-17585	bulloides	15063	128

(Continued) UCI refers to the Keck AMS Facility at the University of California at Irvine. Results labeled “NSRL/NOS AMS” were prepared at the INSTAAR Laboratory for AMS Radiocarbon Preparation and Research at University of Colorado, Boulder (along with associated standards and process blanks) and provided as pressed graphite targets for measurement at the National Ocean Sciences AMS Facility at the Woods Hole Oceanographic Institution. NOSAMS-reported results were $\delta^{13}\text{C}$ - and blank-corrected at NSRL. Results labeled “NSRL/UCI” were prepared at INSTAAR (along with associated standards and process blanks) and provided as pressed graphite for measurement and $\delta^{13}\text{C}$ - and blank-correction at UCI.

Cariaco ¹⁴ C age	Cariaco ¹⁴ C age (res corr)	Cariaco ¹⁴ C ±	Comments	Deleted	CB_Hulu calendar age (yr BP)	Cal age ±	Cariaco average ¹⁴ C age (420 yr res corr)	¹⁴ C ±	Cariaco avg $\Delta^{14}\text{C}$	$\Delta^{14}\text{C}$ ±
605	185	30			13563	137	11750	45	195	7
1340	920	30			13693	139	11900	30	191	4
1580	1160	50			13822	138	11945	45	203	7
1700	1280	30			13948	136	12050	35	206	5
2720	2300	40			14072	132	12113	43	214	6
3650	3230	30			14193	126	12215	30	217	5
4840	4420	40			14312	120	12335	48	216	7
6320	5900	40			14428	114	12355	25	230	4
7660	7240	40			14541	110	12330	43	251	7
8440	8020	55			14652	108	12470	100	246	16
9040	8620	40			14759	110	12490	40	259	6
9700	9280	45			14863	115	12468	33	279	5
10060	9640	40			14964	121	12610	40	272	6
10440	10020	45		X (c)	15063	128	12618	33	286	5
10200	9780	40			15159	134	12688	33	289	5
10650	10230	55		X (a)	15254	138	12900	60	270	9
10095	9675	25		X (a)	15347	141	12840	40	294	6
11900	11480	70	duplicate	X (a)	15438	141	12930	40	294	6
11855	11435	25	duplicate	X (a)	15528	140	12960	40	303	6
12005	11585	30		X (a)	15617	136	13090	40	296	6
12310	11890	50	duplicate	X (a)	15705	130	13040	40	318	7
12220	11800	35	duplicate	X (a)	15792	123	13135	40	317	7
12105	11685	35		X (a)	15878	114	13082	35	339	6
12210	11790	50	duplicate		16133	85	13130	35	373	6
12130	11710	40	duplicate		16217	79	13080	40	396	7
12320	11900	30			16300	76	13290	55	373	9
12530	12110	55	duplicate		16383	77	13170	40	408	7
12200	11780	35	duplicate		16464	80	13323	43	395	7
12470	12050				16544	85	13060	50	456	9
12590	12170	55	duplicate		16700	93	13320	50	436	9
12475	12055	30	duplicate		16849	96	13320	40	462	7
12635	12215				16920	95	13365	45	467	8
12800	12380	65	duplicate		16990	94	13370	40	478	7
12710	12290	30	duplicate		17123	92	13490	40	480	7
12775	12355	25			17185	93	13583	45	474	8
12700	12280	55	duplicate		17246	96	13567	38	488	7
12800	12380	30	duplicate		17305	100	13980	42	423	7
12440	12020	25	duplicate	X (b)	17363	103	13750	25	475	5
12890	12470	100	duplicate		17420	104	14060	30	429	5
12840	12420	40	duplicate		17477	105	14145	25	424	4
12980	12560	40	duplicate		17534	104	14110	50	440	9
12885	12465	25	duplicate		17592	102	14215	25	431	4
12890	12470	40	duplicate		17650	100	14245	55	436	10
13030	12610	40			17710	99	14125	30	468	5
12985	12565	25	duplicate		17772	100	14365	25	435	4

Table 1 (Continued)

ODP Hole	Section	Upper depth	Lower depth	Composite depth (mbsf)	Adjusted depth (mbsf)	AMS lab ID#	Species	CB_Hulu calendar age (yr BP)	Cal age \pm
1002D	2 H 1	95	97.5	5.663	5.66	CAMS-59352	ruber	15063	128
1002D	2 H 1	100	102.5	5.713	5.71	UCIAMS-17586	bulloides	15159	134
1002D	2 H 1	100	102.5	5.713	5.71	CAMS-59353	ruber	15159	134
1002D	2 H 1	105	107.5	5.763	5.76	CAMS-59354	ruber	15254	138
1002D	2 H 1	110	112.5	5.813	5.81	CAMS-59355	ruber	15347	141
1002D	2 H 1	115	117.5	5.863	5.86	CAMS-60321	ruber	15438	141
1002D	2 H 1	120	122.5	5.913	5.91	CAMS-59356	ruber	15528	140
1002D	2 H 1	125	127.5	5.963	5.96	CAMS-59357	ruber	15617	136
1002D	2 H 1	130	132.5	6.013	6.01	CAMS-53785	ruber	15705	130
1002D	2 H 1	135	137.5	6.063	6.06	UCIAMS-15432	ruber	15792	123
1002D	2 H 1	135	137.5	6.063	6.06	UCIAMS-15404	ruber	15792	123
1002D	2 H 1	135	137.5	6.063	6.06	NSRL-13056	bulloides	15792	123
1002D	2 H 1	140	142.5	6.113	6.11	UCIAMS-15433	ruber	15878	114
1002D	2 H 1	140	142.5	6.113	6.11	CAMS-59358	ruber	15878	114
1002D	2 H 1	140	142.5	6.113	6.11	UCIAMS-15405	ruber	15878	114
1002D	2 H 2	0	2.5	6.213	6.21	CAMS-59359	ruber	16048	94
1002D	2 H 2	5	7.5	6.263	6.26	NSRL-13057	ruber	16133	85
1002D	2 H 2	5	7.5	6.263	6.26	UCIAMS-13023	ruber	16133	85
1002D	2 H 2	10	12.5	6.313	6.31	CAMS-59360	ruber	16217	79
1002D	2 H 2	15	17.5	6.363	6.36	UCIAMS-15406	ruber	16300	76
1002D	2 H 2	15	17.5	6.363	6.36	NSRL-13058	bulloides	16300	76
1002D	2 H 2	20	22.5	6.413	6.41	CAMS-59361	ruber	16383	77
1002D	2 H 2	25	27.5	6.463	6.46	UCIAMS-15407	ruber	16464	80
1002D	2 H 2	25	27.5	6.463	6.46	NSRL-13059	bulloides	16464	80
1002D	2 H 2	30	32.5	6.513	6.51	UCIAMS-15408	mixed	16544	85
1002D	2 H 2	30	32.5	6.513	6.51	CAMS-53786	ruber	16544	85
1002D	2 H 2	35	37.5	6.563	6.56	NSRL-13060	mixed	16623	90
1002D	2 H 2	40	42.5	6.613	6.61	UCIAMS-15409	mixed	16700	93
1002D	2 H 2	40	42.5	6.613	6.61	CAMS-59362	ruber	16700	93
1002D	2 H 2	50	52.5	6.713	6.71	CAMS-59363	ruber	16849	96
1002D	2 H 2	55	57.5	6.763	6.76	UCIAMS-15410	ruber	16920	95
1002D	2 H 2	55	57.5	6.763	6.76	NSRL-13062	bulloides	16920	95
1002D	2 H 2	60	62.5	6.813	6.81	CAMS-59364	ruber	16990	94
1002D	2 H 2	70	72.5	6.913	6.91	CAMS-59365	ruber	17123	92
1002D	2 H 2	75	77.5	6.963	6.96	NSRL-13063	bulloides	17185	93
1002D	2 H 2	75	77.5	6.963	6.96	UCIAMS-15411	ruber	17185	93
1002D	2 H 2	80	82.5	7.013	7.01	UCIAMS-17587	ruber	17246	96
1002D	2 H 2	80	82.5	7.013	7.01	UCIAMS-15412	ruber	17246	96
1002D	2 H 2	80	82.5	7.013	7.01	CAMS-53787	ruber	17246	96
1002D	2 H 2	85	87.5	7.063	7.06	UCIAMS-13792	ruber	17305	100
1002D	2 H 2	85	87.5	7.063	7.06	NSRL-13064	bulloides	17305	100
1002D	2 H 2	85	87.5	7.063	7.06	UCIAMS-21419	ruber	17305	100
1002D	2 H 2	90	92.5	7.113	7.11	UCIAMS-15417	bulloides	17363	103
1002D	2 H 2	90	92.5	7.113	7.11	UCIAMS-16533	ruber	17363	103
1002D	2 H 2	95	97.5	7.163	7.16	UCIAMS-13793	ruber	17420	104
1002D	2 H 2	95	97.5	7.163	7.16	NSRL-13065	bulloides	17420	104
1002D	2 H 2	100	102.5	7.213	7.21	UCIAMS-15418	bulloides	17477	105
1002D	2 H 2	105	107.5	7.263	7.26	NSRL-12275	bulloides	17534	104
1002D	2 H 2	105	107.5	7.263	7.26	UCIAMS-21420	ruber	17534	104
1002D	2 H 2	110	112.5	7.313	7.31	UCIAMS-15419	bulloides	17592	102
1002D	2 H 2	115	117.5	7.363	7.36	UCIAMS-15420	ruber	17650	100

Cariaco ¹⁴ C age	Cariaco ¹⁴ C age (res corr)	Cariaco ¹⁴ C ±	Comments	Deleted	CB_Hulu calendar age (yr BP)	Cal age ±	Cariaco average ¹⁴ C age (420 yr res corr)	¹⁴ C ±	Cariaco avg Δ ¹⁴ C	Δ ¹⁴ C ±
13090	12670	40	duplicate		17836	103	14462	43	429	8
13055	12635	25	duplicate		17902	108	14500	35	434	6
13160	12740	40	duplicate		17970	112	14590	57	430	7
13320	12900	60			18041	115	15135	25	347	4
13260	12840	40			18115	117	15128	30	361	5
13350	12930	40			18192	118	15210	30	360	5
13380	12960	40			18273	117	14865	53	433	9
13510	13090	40			18356	114	14870	30	447	5
13460	13040	40			18444	110	15283	53	389	9
13465	13045	35	triplicate		18535	106	15320	30	398	5
13500	13080	25	triplicate		18671	101	15630	45	367	8
13700	13280	60	triplicate		18700	101	15530	50	389	9
13440	13020	40	triplicate		18837	101	15743	50	375	9
13510	13090	40	triplicate		18947	106	15980	25	353	4
13555	13135	25	triplicate		19061	111	16015	60	366	10
14020	13600	260		X (b)	19179	118	16070	30	376	5
13200	12780	130	duplicate	X (c)	19300	123	16090	38	393	7
13550	13130	35	duplicate		19423	128	16260	40	384	7
13500	13080	40			19548	131	16403	58	381	10
13620	13200	30	duplicate		19674	131	16280	35	424	6
13800	13380	80	duplicate		19801	130	16370	50	430	9
13590	13170	40			19929	127	16525	60	424	11
13635	13215	25	duplicate		20056	123	16540	35	443	6
13850	13430	60	duplicate		20183	118	16690	55	439	10
12625	12205	35	duplicate	X (b)	20308	113	16685	35	461	6
13480	13060	50	duplicate		20431	109	16685	58	483	11
13250	12830	65		X (c)	20552	109	16940	35	458	6
12600	12180	35	duplicate	X (b)	20671	113	17090	58	452	10
13740	13320	50	duplicate		20786	121	17025	35	484	6
13740	13320	40			20899	132	17340	38	447	7
13770	13350	25	duplicate		21009	144	17280	55	477	10
13800	13380	65	duplicate		21118	156	17398	40	475	7
13790	13370	40			21224	168	17303	35	512	7
13910	13490	40			21328	179	17615	38	473	7
14000	13580	60	duplicate		21431	189	17490	30	514	6
14005	13585	30	duplicate		21532	197	17430	110	545	21
13855	13435	30	triplicate		21632	203	17620	35	527	7
14035	13615	25	triplicate		21730	208	17540	90	561	17
14070	13650	60	triplicate		21827	211	17730	40	542	8
14350	13930	30	triplicate		21923	212	17850	40	537	8
14500	14080	65	triplicate		22018	211	17895	65	546	13
14350	13930	30	triplicate		22113	209	17985	35	546	7
14110	13690	25	duplicate		22206	205	18140	80	534	15
14230	13810	25	duplicate		22299	200	18260	40	528	8
14480	14060	30	duplicate		22392	193	18440	45	511	8
14650	14230	70	duplicate	X (c)	22483	186	18430	100	530	19
14565	14145	25			22575	178	18210	40	590	8
14400	13980	70	duplicate		22666	171	18315	50	587	10
14660	14240	30	duplicate		22757	165	18505	40	567	8
14635	14215	25			22847	160	18293	38	627	8
14580	14160	25	duplicate		22938	159	18757	45	552	9

Table 1 (Continued)

ODP Hole	Section	Upper depth	Lower depth	Composite depth (mbsf)	Adjusted depth (mbsf)	AMS lab ID#	Species	CB_Hulu calendar age (yr BP)	Cal age \pm
1002D	2 H 2	115	117.5	7.363	7.36	NSRL-13066	bulloides	17650	100
1002D	2 H 2	120	122.5	7.413	7.41	UCIAMS-15421	bulloides	17710	99
1002D	2 H 2	125	127.5	7.463	7.46	UCIAMS-15422	bulloides	17772	100
1002D	2 H 2	125	127.5	7.463	7.46	NSRL-13067	bulloides	17772	100
1002D	2 H 2	130	132.5	7.513	7.51	CAMS-52121	bulloides	17836	103
1002D	2 H 2	130	132.5	7.513	7.51	UCIAMS-13794	ruber	17836	103
1002D	2 H 2	130	132.5	7.513	7.51	CAMS-54468	ruber	17836	103
1002D	2 H 2	135	137.5	7.563	7.56	UCIAMS-15423	ruber	17902	108
1002D	2 H 2	140	142.5	7.613	7.61	UCIAMS-13024	ruber	17970	112
1002D	2 H 2	140	142.5	7.613	7.61	UCIAMS-13069	ruber	17970	112
1002D	2 H 2	140	142.5	7.613	7.61	NSRL-13068	bulloides	17970	112
1002D	2 H 2	145	147.5	7.663	7.66	UCIAMS-15424	ruber	18041	115
1002D	2 H 3	0	2.5	7.713	7.71	UCIAMS-13070	ruber	18115	117
1002D	2 H 3	0	2.5	7.713	7.71	UCIAMS-13025	ruber	18115	117
1002D	2 H 3	0	2.5	7.713	7.71	NSRL-13069	bulloides	18115	117
1002D	2 H 3	5	7.5	7.763	7.76	UCIAMS-15429	ruber	18192	118
1002D	2 H 3	10	12.5	7.813	7.81	NSRL-12276	bulloides	18273	117
1002D	2 H 3	10	12.5	7.813	7.81	UCIAMS-13795	ruber	18273	117
1002D	2 H 3	15	17.5	7.863	7.86	UCIAMS-15430	ruber	18356	114
1002D	2 H 3	20	22.5	7.913	7.91	UCIAMS-16934	ruber	18444	110
1002D	2 H 3	20	22.5	7.913	7.91	NSRL-13070	bulloides	18444	110
1002D	2 H 3	20	22.5	7.913	7.91	UCIAMS-21421	ruber	18444	110
1002D	2 H 3	25	27.5	7.963	7.96	UCIAMS-15431	bulloides	18535	106
1002D	2 H 3	30	32.5	8.027	8.03	CAMS-52770	ruber	18671	101
1002D	2 H 3	30	32.5	8.027	8.03	CAMS-52122	bulloides	18671	101
1002D	2 H 3	30	32.5	8.031	8.03	CAMS-53788	ruber	18671	101
1002D	2 H 3	40	42.5	8.113	8.11	NSRL-13071	bulloides	18837	101
1002D	2 H 3	40	42.5	8.113	8.11	UCIAMS-16935	ruber	18837	101
1002D	2 H 3	45	47.5	8.163	8.16	UCIAMS-16936	ruber	18947	106
1002D	2 H 3	50	52.5	8.213	8.21	UCIAMS-16937	ruber	19061	111
1002D	2 H 3	50	52.5	8.213	8.21	NSRL-13072	bulloides	19061	111
1002D	2 H 3	55	57.5	8.263	8.26	UCIAMS-13796	ruber	19179	118
1002D	2 H 3	60	62.5	8.313	8.31	NSRL-12277	bulloides	19300	123
1002D	2 H 3	60	62.5	8.313	8.31	UCIAMS-13071	ruber	19300	123
1002D	2 H 3	60	62.5	8.313	8.31	UCIAMS-13026	ruber	19300	123
1002D	2 H 3	65	67.5	8.363	8.36	UCIAMS-13797	ruber	19423	128
1002D	2 H 3	70	72.5	8.413	8.41	NSRL-13073	bulloides	19548	131
1002D	2 H 3	70	72.5	8.413	8.41	UCIAMS-16938	ruber	19548	131
1002D	2 H 3	75	77.5	8.463	8.46	UCIAMS-13798	ruber	19674	131
1002D	2 H 3	80	82.5	8.513	8.51	CAMS-52123	bulloides	19801	130
1002D	2 H 3	80	82.5	8.513	8.51	CAMS-53789	bulloides	19801	130
1002D	2 H 3	80	82.5	8.513	8.51	CAMS-52771	ruber	19801	130
1002D	2 H 3	85	87.5	8.563	8.56	UCIAMS-16939	ruber	19929	127
1002D	2 H 3	85	87.5	8.563	8.56	NSRL-13074	bulloides	19929	127
1002D	2 H 3	90	92.5	8.613	8.61	UCIAMS-16534	bulloides	20056	123
1002D	2 H 3	95	97.5	8.663	8.66	UCIAMS-16940	ruber	20183	118
1002D	2 H 3	95	97.5	8.663	8.66	NSRL-13075	bulloides	20183	118
1002D	2 H 3	100	102.5	8.713	8.71	UCIAMS-16535	bulloides	20308	113
1002D	2 H 3	105	107.5	8.763	8.76	NSRL-12278	bulloides	20431	109
1002D	2 H 3	105	107.5	8.763	8.76	UCIAMS-13799	ruber	20431	109

Cariaco ¹⁴ C age	Cariaco ¹⁴ C age (res corr)	Cariaco ¹⁴ C ±	Comments	Deleted	CB_Hulu calendar age (yr BP)	Cal age ±	Cariaco average ¹⁴ C age (420 yr res corr)	¹⁴ C ±	Cariaco avg Δ ¹⁴ C	Δ ¹⁴ C ±
14750	14330	85	duplicate		23029	160	18918	70	538	13
14545	14125	30			23119	162	18875	35	563	7
14785	14365	25	duplicate		23209	166	19095	75	538	14
15100	14680	70	duplicate	X (c)	23300	171	18940	40	585	8
14750	14330	40	triplicate		23390	174	19180	90	555	17
14905	14485	30	triplicate		23479	177	19275	40	554	8
14990	14570	60	triplicate		23569	179	18960	43	633	9
14920	14500	35			23658	180	19525	45	539	9
14960	14540	30	triplicate		23747	178	19680	95	526	18
15060	14640	45	triplicate		23836	175	19785	60	522	11
15750	15330	95	triplicate	X (c)	23924	170	19880	90	521	17
15555	15135	25			24012	164	19790	45	554	9
15490	15070	30	triplicate		24099	156	19835	73	562	14
15605	15185	30	triplicate		24186	147	20258	38	498	7
16150	15730	70	triplicate	X (c)	24272	138	20195	70	525	13
15630	15210	30			24358	128	20023	48	574	9
15200	14780	75	duplicate		24443	119	20315	65	534	12
15370	14950	30	duplicate		24527	111	20275	45	557	9
15290	14870	30			24611	107	20345	35	559	7
15695	15275	25	triplicate		24694	105	20490	60	547	12
15800	15380	95	triplicate		24777	106	20585	40	544	8
15615	15195	40	triplicate		24859	107	20600	45	557	9
15740	15320	30			24940	108	20763	55	541	11
16020	15600	50	duplicate		25022	108	20828	65	543	12
16080	15660	40	duplicate		25103	107	21145	80	498	15
15950	15530	50			25184	106	21230	50	497	9
16150	15730	70	duplicate		25265	105	21230	45	512	8
16175	15755	30	duplicate		25347	106	21228	80	527	15
16400	15980	25			25428	110	21330	50	523	9
16370	15950	25	duplicate		25510	117	21470	70	511	13
16500	16080	95	duplicate		25593	126	21515	40	518	8
16490	16070	30			25676	137	21483	53	540	10
15700	15280	100	triplicate	X (b)	25760	148	21760	40	502	7
16400	15980	40	triplicate		25843	159	21725	45	524	9
16620	16200	35	triplicate		25928	169	22240	83	444	15
16680	16260	40			26013	178	22105	40	484	7
16800	16380	90	duplicate		26098	186	22100	83	500	15
16845	16425	25	duplicate		26184	192	22028	43	530	8
16700	16280	35			26271	196	22340	50	506	9
16230	15810	40	triplicate	X (b)	26359	198	22343	105	502	20
16770	16350	50	triplicate		26447	199	22783	48	438	9
16810	16390	50	triplicate		26536	198	22545	105	497	20
16890	16470	30	duplicate		26626	195	22455	40	530	8
17000	16580	90	duplicate		26717	191	22470	45	544	9
16960	16540	35			26809	185	22588	60	539	11
17070	16650	25	duplicate		26903	178	22540	50	566	10
17150	16730	85	duplicate		26998	170	23295	170	442	22
17105	16685	35			27094	162	22760	65	559	13
17050	16630	80	duplicate		27192	154	23010	50	529	10
17160	16740	35	duplicate		27232	151	23380	150	467	27

Table 1 (Continued)

ODP Hole	Section	Upper depth	Lower depth	Composite depth (mbsf)	Adjusted depth (mbsf)	AMS lab ID#	Species	CB_Hulu calendar age (yr BP)	Cal age \pm
1002D	2 H 3	110	112.5	8.813	8.81	UCIAMS-13804	ruber	20552	109
1002D	2 H 3	115	117.5	8.863	8.86	UCIAMS-16941	ruber	20671	113
1002D	2 H 3	115	117.5	8.863	8.86	NSRL-13076	bulloides	20671	113
1002D	2 H 3	120	122.5	8.913	8.91	UCIAMS-13805	ruber	20786	121
1002D	2 H 3	125	127.5	8.963	8.96	UCIAMS-13072	ruber	20899	132
1002D	2 H 3	125	127.5	8.963	8.96	UCIAMS-13027	ruber	20899	132
1002D	2 H 3	125	127.5	8.963	8.96	NSRL-13077	bulloides	20899	132
1002D	2 H 3	130	132.5	9.013	9.01	CAMS-52124	bulloides	21009	144
1002D	2 H 3	130	132.5	9.013	9.01	CAMS-53790	bulloides	21009	144
1002D	2 H 3	135	137.5	9.063	9.06	UCIAMS-13029	ruber	21118	156
1002D	2 H 3	135	137.5	9.063	9.06	UCIAMS-13073	ruber	21118	156
1002D	2 H 3	135	137.5	9.063	9.06	NSRL-13078	bulloides	21118	156
1002D	2 H 3	140	142.5	9.113	9.11	UCIAMS-16536	bulloides	21224	168
1002D	2 H 3	140	142.5	9.113	9.11	UCIAMS-13806	ruber	21224	168
1002D	2 H 3	145	147.5	9.163	9.16	UCIAMS-13074	ruber	21328	179
1002D	2 H 3	145	147.5	9.163	9.16	UCIAMS-13030	ruber	21328	179
1002D	2 H 3	145	147.5	9.163	9.16	NSRL-13079	bulloides	21328	179
1002D	2 H 4	0	2.5	9.213	9.21	UCIAMS-16537	bulloides	21431	189
1002D	2 H 4	5	7.5	9.263	9.26	NSRL-12279	bulloides	21532	197
1002D	2 H 4	10	12.5	9.313	9.31	UCIAMS-17574	ruber	21632	203
1002D	2 H 4	15	17.5	9.363	9.36	UCIAMS-3443	bulloides	21730	208
1002D	2 H 4	20	22.5	9.413	9.41	UCIAMS-19506	ruber	21827	211
1002D	2 H 4	25	27.5	9.463	9.46	UCIAMS-17579	ruber	21923	212
1002D	2 H 4	30	32.5	9.513	9.51	CAMS-52125	bulloides	22018	211
1002D	2 H 4	30	32.5	9.513	9.51	CAMS-53791	bulloides	22018	211
1002D	2 H 4	35	37.5	9.563	9.56	UCIAMS-19507	ruber	22113	209
1002D	2 H 4	40	42.5	9.613	9.61	UCIAMS-3444	bulloides	22206	205
1002D	2 H 4	45	47.5	9.663	9.66	UCIAMS-19508	ruber	22299	200
1002D	2 H 4	50	52.5	9.713	9.71	UCIAMS-19509	ruber	22392	193
1002D	2 H 4	55	57.5	9.763	9.76	NSRL-12280	bulloides	22483	186
1002D	2 H 4	55	57.5	9.763	9.76	UCIAMS-21422	ruber	22483	186
1002D	2 H 4	60	62.5	9.813	9.81	UCIAMS-19510	ruber	22575	178
1002D	2 H 4	65	67.5	9.863	9.86	UCIAMS-3445	mixed	22666	171
1002D	2 H 4	65	67.5	9.863	9.86	UCIAMS-13807	ruber	22666	171
1002D	2 H 4	70	72.5	9.913	9.91	UCIAMS-19511	ruber	22757	165
1002D	2 H 4	70	72.5	9.913	9.91	UCIAMS-21423	ruber	22757	165
1002D	2 H 4	75	77.5	9.963	9.96	UCIAMS-13808	ruber	22847	160
1002D	2 H 4	75	77.5	9.963	9.96	UCIAMS-21424	ruber	22847	160
1002D	2 H 4	80	82.5	10.013	10.01	CAMS-52126	bulloides	22938	159
1002D	2 H 4	80	82.5	10.013	10.01	UCIAMS-13809	ruber	22938	159
1002D	2 H 4	80	82.5	10.013	10.01	CAMS-53792	bulloides	22938	159
1002D	2 H 4	80	82.5	10.013	10.01	UCIAMS-21425	ruber	22938	159
1002D	2 H 4	85	87.5	10.063	10.06	NSRL-13137	bulloides	23029	160
1002D	2 H 4	85	87.5	10.063	10.06	UCIAMS-19512	ruber	23029	160
1002D	2 H 4	90	92.5	10.113	10.11	UCIAMS-17580	ruber	23119	162
1002D	2 H 4	95	97.5	10.163	10.16	NSRL-13138	bulloides	23209	166
1002D	2 H 4	95	97.5	10.163	10.16	UCIAMS-19513	ruber	23209	166
1002D	2 H 4	100	102.5	10.213	10.21	UCIAMS-19514	ruber	23300	171
1002D	2 H 4	105	107.5	10.263	10.26	NSRL-12281	bulloides	23390	174
1002D	2 H 4	110	112.5	10.313	10.31	UCIAMS-13810	ruber	23479	177

Cariaco ¹⁴ C age	Cariaco ¹⁴ C age (res corr)	Cariaco ¹⁴ C ±	Comments	Deleted	CB_Hulu calendar age (yr BP)	Cal age ±	Cariaco average ¹⁴ C age (420 yr res corr)	¹⁴ C ±	Cariaco avg $\Delta^{14}\text{C}$	$\Delta^{14}\text{C}$ ±
17360	16940	35			27292	146	23330	70	487	13
17420	17000	25	duplicate		27395	138	23515	100	472	18
17600	17180	90	duplicate		27500	130	23220	60	546	12
17445	17025	35			27588	124	23980	170	422	30
17730	17310	40	triplicate		27610	122	23130	70	585	14
17790	17370	35	triplicate		27724	115	24140	70	417	12
18200	17780	100	triplicate	X (c)	27771	112	24080	190	436	34
17630	17210	60	duplicate		27843	108	23880	140	485	26
17770	17350	50	duplicate		27968	103	24160	60	456	11
17780	17360	35	triplicate		28072	100	23980	140	508	26
17855	17435	45	triplicate		28099	100	24020	90	505	17
18100	17680	130	triplicate	X (c)	28236	100	24160	60	504	11
17690	17270	35	duplicate		28378	101	24280	150	507	28
17755	17335	35	duplicate		28378	101	24070	100	547	19
18010	17590	40	triplicate		28523	103	24140	80	561	16
18060	17640	35	triplicate		28552	103	24180	130	558	25
18550	18130	140	triplicate	X (c)	28668	106	24070	70	602	14
17910	17490	30			28812	111	24410	60	563	12
17850	17430	110			28953	117	24518	95	569	19
18040	17620	35			29090	126	24420	60	614	12
17960	17540	90			29195	136	25065	95	509	18
18150	17730	40			29346	154	25060	140	538	27
18270	17850	40			29419	163	25130	120	538	23
18250	17830	80	duplicate		29466	170	24260	150	723	32
18380	17960	50	duplicate		29582	187	25040	140	586	28
18405	17985	35			29627	194	25330	100	538	19
18560	18140	80			29693	204	25100	150	595	30
18680	18260	40			29800	222	25590	210	520	40
18860	18440	45			29862	232	25980	140	459	25
18850	18430	100	duplicate		29903	239	25580	170	542	33
18395	17975	45	duplicate	X (d)	30003	255	25190	150	638	31
18630	18210	40			30099	271	25980	180	502	34
18680	18260	60	duplicate		30099	271	25900	180	517	34
18790	18370	40	duplicate		30193	286	26180	180	482	33
18960	18540	40	duplicate		30303	302	25880	140	559	27
18890	18470	40	duplicate		30496	327	25880	180	595	36
18735	18315	35	duplicate		30547	333	25730	160	636	33
18690	18270	40	duplicate		30664	345	26250	80	555	15
18910	18490	60	quadruplicate	X (d)	30681	347	25950	90	617	18
19150	18730	45	quadruplicate		30697	348	25980	140	615	28
19250	18830	50	quadruplicate		30763	354	25940	180	636	37
19130	18710	40	quadruplicate		30812	357	26480	150	538	29
19450	19030	100	duplicate		30844	359	26310	170	577	33
19225	18805	40	duplicate		30861	360	26380	170	567	33
19295	18875	35			30957	364	26950	70	477	13
19550	19130	110	duplicate		31038	366	27180	210	449	38
19480	19060	40	duplicate		31134	367	26920	110	514	21
19360	18940	40			31231	365	27080	230	502	43
19600	19180	90			31329	362	27675	145	411	25
19695	19275	40			31462	354	27800	155	412	27

Table 1 (Continued)

ODP Hole	Section	Upper depth	Lower depth	Composite depth (mbsf)	Adjusted depth (mbsf)	AMS lab ID#	Species	CB_Hulu calendar age (yr BP)	Cal age \pm
1002D	2 H 4	115	117.5	10.363	10.36	NSRL-13139	bulloides	23569	179
1002D	2 H 4	115	117.5	10.363	10.36	UCIAMS-13075	ruber	23569	179
1002D	2 H 4	115	117.5	10.363	10.36	UCIAMS-13031	ruber	23569	179
1002D	2 H 4	120	122.5	10.413	10.41	UCIAMS-13811	ruber	23658	180
1002D	2 H 4	125	127.5	10.463	10.46	NSRL-13140	bulloides	23747	178
1002D	2 H 4	130	132.5	10.513	10.51	CAMS-52127	bulloides	23836	175
1002D	2 H 4	130	132.5	10.513	10.51	CAMS-53793	bulloides	23836	175
1002D	2 H 4	135	137.5	10.563	10.56	NSRL-13141	bulloides	23924	170
1002D	2 H 4	135	137.5	10.563	10.56	UCIAMS-21426	ruber	23924	170
1002D	2 H 4	140	142.5	10.613	10.61	UCIAMS-17566	ruber	24012	164
1002D	2 H 4	145	147.5	10.663	10.66	NSRL-13142	bulloides	24099	156
1002D	2 H 4	145	147.5	10.663	10.66	UCIAMS-17567	ruber	24099	156
1002D	2 H 5	0	2.5	10.713	10.71	UCIAMS-17568	ruber	24186	147
1002D	2 H 5	0	2.5	10.713	10.71	UCIAMS-19519	ruber	24186	147
1002D	2 H 5	5	7.5	10.763	10.76	NSRL-12282	bulloides	24272	138
1002D	2 H 5	5	7.5	10.763	10.76	UCIAMS-17569	ruber	24272	138
1002D	2 H 5	10	12.5	10.813	10.81	UCIAMS-16538	bulloides	24358	128
1002D	2 H 5	10	12.5	10.813	10.81	UCIAMS-21427	ruber	24358	128
1002D	2 H 5	15	17.5	10.863	10.86	UCIAMS-16947	ruber	24443	119
1002D	2 H 5	15	17.5	10.863	10.86	NSRL-13080	bulloides	24443	119
1002D	2 H 5	20	22.5	10.913	10.91	UCIAMS-16539	bulloides	24527	111
1002D	2 H 5	25	27.5	10.963	10.96	UCIAMS-16948	ruber	24611	107
1002D	2 H 5	25	27.5	10.963	10.96	NSRL-13081	bulloides	24611	107
1002D	2 H 5	30	32.5	11.013	11.01	CAMS-52754	bulloides	24694	105
1002D	2 H 5	35	37.5	11.063	11.06	UCIAMS-16949	ruber	24777	106
1002D	2 H 5	35	37.5	11.063	11.06	NSRL-13082	bulloides	24777	106
1002D	2 H 5	40	42.5	11.113	11.11	UCIAMS-16543	bulloides	24859	107
1002D	2 H 5	45	47.5	11.163	11.16	UCIAMS-16950	ruber	24940	108
1002D	2 H 5	45	47.5	11.163	11.16	NSRL-13083	bulloides	24940	108
1002D	2 H 5	45	47.5	11.163	11.16	UCIAMS-19520	ruber	24940	108
1002D	2 H 5	45	47.5	11.163	11.16	UCIAMS-21431	bulloides	24940	108
1002D	2 H 5	50	52.5	11.213	11.21	UCIAMS-16545	bulloides	25022	108
1002D	2 H 5	50	52.5	11.213	11.21	UCIAMS-21432	ruber	25022	108
1002D	2 H 5	55	57.5	11.263	11.26	NSRL-12283	bulloides	25103	107
1002D	2 H 5	55	57.5	11.263	11.26	UCIAMS-21433	ruber	25103	107
1002D	2 H 5	60	62.5	11.313	11.31	UCIAMS-16546	bulloides	25184	106
1002D	2 H 5	60	62.5	11.313	11.31	UCIAMS-19521	ruber	25184	106
1002D	2 H 5	60	62.5	11.313	11.31	UCIAMS-21434	ruber	25184	106
1002D	2 H 5	65	67.5	11.363	11.36	UCIAMS-16547	bulloides	25265	105
1002D	2 H 5	65	67.5	11.363	11.36	UCIAMS-19522	ruber	25265	105
1002D	2 H 5	65	67.5	11.363	11.36	UCIAMS-21435	ruber	25265	105
1002D	2 H 5	70	72.5	11.413	11.41	UCIAMS-16951	ruber	25347	106
1002D	2 H 5	70	72.5	11.413	11.41	NSRL-13084	bulloides	25347	106
1002D	2 H 5	75	77.5	11.463	11.46	UCIAMS-16548	bulloides	25428	110
1002D	2 H 5	80	82.5	11.513	11.51	CAMS-52755	bulloides	25510	117
1002D	2 H 5	85	87.5	11.563	11.56	UCIAMS-16952	ruber	25593	126
1002D	2 H 5	90	92.5	11.613	11.61	UCIAMS-3446	bulloides	25676	137
1002D	2 H 5	90	92.5	11.613	11.61	UCIAMS-19523	ruber	25676	137
1002D	2 H 5	90	92.5	11.613	11.61	UCIAMS-21436	ruber	25676	137
1002D	2 H 5	95	97.5	11.663	11.66	UCIAMS-16953	ruber	25760	148

Cariaco ¹⁴ C age	Cariaco ¹⁴ C age (res corr)	Cariaco ¹⁴ C ±	Comments	Deleted	CB_Hulu calendar age (yr BP)	Cal age ±	Cariaco average ¹⁴ C age (420 yr res corr)	¹⁴ C ±	Cariaco avg Δ ¹⁴ C	Δ ¹⁴ C ±
19200	18780	110	triplicate	X (d)	31615	340	27840	130	442	23
19350	18930	40	triplicate		31720	329	27980	180	425	32
19410	18990	45	triplicate		31811	318	28280	210	387	36
19945	19525	45			31866	311	28180	190	414	33
20100	19680	95			32160	271	28060	230	487	43
20160	19740	60	duplicate		32421	237	27980	180	550	35
20250	19830	60	duplicate		32514	228	28080	270	549	52
20400	19980	130	duplicate		32561	223	28590	140	462	25
20200	19780	50	duplicate		32610	219	27480	220	688	46
20210	19790	35			32635	218	28530	110	486	20
20200	19780	95	duplicate		32660	216	28290	130	536	25
20310	19890	50	duplicate		32736	212	28280	160	552	31
20720	20300	40	duplicate		32736	212	28650	160	482	30
20635	20215	35	duplicate		32866	209	28650	110	505	21
20600	20180	100	duplicate		32893	209	28480	170	543	33
20630	20210	40	duplicate		33000	210	28570	80	545	15
20445	20025	35	duplicate		33110	212	28580	230	564	45
20440	20020	60	duplicate		33137	213	28860	110	515	21
20670	20250	35	duplicate		33248	218	28970	80	515	15
20800	20380	95	duplicate		33386	225	29170	240	503	45
20695	20275	45			33525	231	28990	110	563	21
20765	20345	35	duplicate		33662	236	29260	110	536	21
21250	20830	120	duplicate	X (c)	33769	238	29270	170	554	33
20910	20490	60			33901	239	29050	105	623	21
21005	20585	40	duplicate		34153	233	29520	150	578	29
21270	20850	130	duplicate	X (c)	34250	231	29610	160	579	31
21020	20600	45			34484	230	29610	210	625	42
21575	21155	35	quadruplicate	X (d)	34688	230	30110	170	565	33
21810	21390	110	quadruplicate	X (c)	34908	231	30380	170	554	33
21225	20805	40	quadruplicate		35015	232	30480	320	555	62
21140	20720	70	quadruplicate		35202	238	30570	100	572	20
21125	20705	50	duplicate		35303	243	30405	230	625	47
21370	20950	80	duplicate		35495	252	31330	250	482	46
21510	21090	100	duplicate		35658	254	31160	180	544	35
21620	21200	60	duplicate		35898	246	31020	140	617	28
21770	21350	50	triplicate		36144	231	31330	180	603	36
21590	21170	40	triplicate		36290	224	31460	260	606	52
21590	21170	60	triplicate		36455	221	31670	240	596	48
22000	21580	70	triplicate	X (d)	36607	222	31910	200	577	39
21625	21205	40	triplicate		36694	225	30890	290	810	65
21675	21255	50	triplicate		36783	227	32110	210	572	41
21595	21175	40	duplicate		36946	230	32140	220	597	44
21700	21280	120	duplicate		37038	230	32310	120	581	24
21750	21330	50			37131	229	32220	280	617	56
21890	21470	70			37206	228	32720	310	533	59
21935	21515	40			37301	225	32480	360	598	72
22320	21900	110	triplicate	X (d)	37396	221	32840	220	546	42
21925	21505	45	triplicate		37491	215	32890	130	554	25
21880	21460	60	triplicate		37568	210	32600	170	626	34
22180	21760	40			37760	196	32840	220	615	44

Table 1 (Continued)

ODP Hole	Section	Upper depth	Lower depth	Composite depth (mbsf)	Adjusted depth (mbsf)	AMS lab ID#	Species	CB_Hulu calendar age (yr BP)	Cal age \pm
1002D	2 H 5	100	102.5	11.713	11.71	UCIAMS-17570	ruber	25843	159
1002D	2 H 5	105	107.5	11.763	11.76	NSRL-12284	bulloides	25928	169
1002D	2 H 5	105	107.5	11.763	11.76	UCIAMS-19524	ruber	25928	169
1002D	2 H 5	110	112.5	11.813	11.81	UCIAMS-16954	ruber	26013	178
1002D	2 H 5	115	117.5	11.863	11.86	UCIAMS-3449	bulloides	26098	186
1002D	2 H 5	115	117.5	11.863	11.86	UCIAMS-19525	ruber	26098	186
1002D	2 H 5	120	122.5	11.913	11.91	UCIAMS-17571	ruber	26184	192
1002D	2 H 5	120	122.5	11.913	11.91	UCIAMS-19526	ruber	26184	192
1002D	2 H 5	125	127.5	11.963	11.96	UCIAMS-16959	ruber	26271	196
1002D	2 H 5	130	132.5	12.013	12.01	CAMS-52756	bulloides	26359	198
1002D	2 H 5	130	132.5	12.013	12.01	UCIAMS-19527	ruber	26359	198
1002D	2 H 5	135	137.5	12.063	12.06	UCIAMS-16960	ruber	26447	199
1002D	2 H 5	135	137.5	12.063	12.06	UCIAMS-19531	ruber	26447	199
1002D	2 H 5	140	142.5	12.113	12.11	UCIAMS-3450	bulloides	26536	198
1002D	2 H 5	140	142.5	12.113	12.11	UCIAMS-19532	ruber	26536	198
1002D	2 H 5	145	147.5	12.163	12.16	UCIAMS-16961	ruber	26626	195
1002D	2 H 6	0	2.5	12.213	12.21	UCIAMS-17572	ruber	26717	191
1002D	2 H 6	5	7.5	12.263	12.26	NSRL-12285	bulloides	26809	185
1002D	2 H 6	5	7.5	12.263	12.26	UCIAMS-19533	ruber	26809	185
1002D	2 H 6	5	7.5	12.263	12.26	UCIAMS-21437	ruber	26809	185
1002D	2 H 6	10	12.5	12.313	12.31	UCIAMS-19534	ruber	26903	178
1002D	2 H 6	15	17.5	12.363	12.36	UCIAMS-3558	bulloides	26998	170
1002D	2 H 6	15	17.5	12.363	12.36	UCIAMS-3451	bulloides	26998	170
1002D	2 H 6	15	17.5	12.363	12.36	UCIAMS-19535	ruber	26998	170
1002D	2 H 6	20	22.5	12.413	12.41	UCIAMS-16962	ruber	27094	162
1002D	2 H 6	20	22.5	12.413	12.41	UCIAMS-21438	ruber	27094	162
1002D	2 H 6	25	27.5	12.463	12.46	UCIAMS-17573	ruber	27192	154
1002E	3 H 1	45	47.5	12.475	12.48	NSRL-13108	bulloides	27232	151
1002D	2 H 6	30	32.5	12.513	12.51	CAMS-52757	bulloides	27292	146
1002E	3 H 1	55	57.5	12.56	12.56	NSRL-13109	bulloides	27395	138
1002D	2 H 6	35	37.5	12.563	12.56	UCIAMS-21439	bulloides	27395	138
1002D	2 H 6	40	42.5	12.613	12.61	UCIAMS-21443	bull+ruber	27500	130
1002E	3 H 1	65	67.5	12.65	12.65	NSRL-13110	bulloides	27588	124
1002D	2 H 6	40	42.5	12.663	12.66	UCIAMS-21444	mixed	27610	122
1002D	2 H 6	40	42.5	12.713	12.71	UCIAMS-21445	ruber	27724	115
1002E	3 H 1	75	77.5	12.73	12.73	NSRL-13111	bulloides	27771	112
1002D	2 H 6	55	57.5	12.763	12.76	NSRL-12286	bulloides	27843	108
1002D	2 H 6	60	62.5	12.813	12.81	UCIAMS-21446	ruber	27968	103
1002E	3 H 1	85	87.5	12.85	12.85	NSRL-13112	bulloides	28072	100
1002D	2 H 6	65	67.5	12.863	12.86	UCIAMS-21447	bulloides	28099	100
1002D	2 H 6	70	72.5	12.913	12.91	UCIAMS-21448	ruber	28236	100
1002E	3 H 1	95	97.5	12.96	12.96	NSRL-13113	bulloides	28378	101
1002D	2 H 6	75	77.5	12.963	12.96	UCIAMS-21449	bulloides	28378	101
1002D	2 H 6	80	82.5	13.013	13.01	CAMS-52758	bulloides	28523	103
1002E	3 H 1	105	107.5	13.02	13.02	NSRL-13114	bulloides	28552	103
1002D	2 H 6	85	87.5	13.063	13.06	CAMS-56891	bulloides	28668	106
1002D	2 H 6	90	92.5	13.113	13.11	CAMS-59627	bulloides	28812	111
1002E	3 H 1	115	117.5	13.16	13.16	NSRL-13115	bulloides	28953	117
1002D	2 H 6	95	97.5	13.163	13.16	UCIAMS-16549	ruber	28953	117

Cariaco ¹⁴ C age	Cariaco ¹⁴ C age (res corr)	Cariaco ¹⁴ C ±	Comments	Deleted	CB_Hulu calendar age (yr BP)	Cal age ±	Cariaco average ¹⁴ C age (420 yr res corr)	¹⁴ C ±	Cariaco avg $\Delta^{14}\text{C}$	$\Delta^{14}\text{C}$ ±
22145	21725	45			37856	188	32940	240	614	48
22670	22250	120	duplicate		38028	174	33280	280	579	55
22650	22230	45	duplicate		38124	167	32840	320	688	67
22525	22105	40			38313	162	33390	240	613	48
22440	22020	120	duplicate		38482	168	33500	180	624	36
22600	22180	45	duplicate		38669	183	33675	260	625	53
22360	21940	40	duplicate		38744	190	33390	345	699	73
22535	22115	45	duplicate		38932	210	33680	300	676	63
22760	22340	50			39027	220	33920	420	646	86
22760	22340	160	duplicate		39199	236	34345	240	594	48
22765	22345	50	duplicate		39395	252	34200	220	662	46
23230	22810	50	duplicate		39576	262	34220	320	694	68
23175	22755	45	duplicate		39893	274	34680	390	663	81
22880	22460	160	duplicate		39980	276	34670	150	682	31
23050	22630	50	duplicate		40201	282	34920	265	675	55
22875	22455	40			40313	284	34600	150	767	33
22890	22470	45			40403	286	34880	210	725	45
23300	22880	130	triplicate	X (d)	40631	289	35380	370	666	77
22945	22525	50	triplicate		40859	290	35460	160	696	34
23070	22650	70	triplicate		40950	289	35980	400	607	80
22960	22540	50			41064	287	36010	320	623	65
23410	22990	120	triplicate		41268	278	36680	500	531	95
23940	23520	350	triplicate		41492	262	36390	260	631	53
23795	23375	50	triplicate		41690	241	37030	340	542	65
23230	22810	70	duplicate		41906	222	37540	290	486	54
23130	22710	60	duplicate		42012	217	37780	430	461	78
23430	23010	50			42096	217	38030	220	430	39
23800	23380	150			42199	219	37590	390	530	74
23750	23330	70			42301	223	38780	520	335	87
24100	23680	120	duplicate		42483	227	38500	350	414	62
23770	23350	80	duplicate		42685	225	39040	460	354	78
23640	23220	60			42977	208	40280	680	202	102
24400	23980	170			43539	155	40070	450	321	74
23550	23130	70			44228	126	40980	640	282	102
24560	24140	70			44889	175	41060	510	375	87
24500	24080	190			45393	231	41230	650	431	116
24300	23880	140			45852	257	43690	700	114	97
24580	24160	60			46313	244	43780	910	164	132
24400	23980	140			46850	201	44220	740	176	109
24440	24020	90			47545	158	45280	1100	121	154
24580	24160	60			48371	157	45920	920	144	131
24700	24280	150			49236	199	46480	1270	185	188
24490	24070	100			49969	282	47080	1100	202	165
24560	24140	80			50589	370	47080	1180	295	191
24600	24180	130			51133	449	46980	1500	401	263
24490	24070	70			51611	512	48780	1720	186	256
24830	24410	60			52081	563	46580	1400	651	289
25100	24680	140			53041	630	48780	1900	410	337
24775	24355	50			53927	650	48780	1900	569	375

Table 1 (Continued)

ODP Hole	Section	Upper depth	Lower depth	Composite depth (mbsf)	Adjusted depth (mbsf)	AMS lab ID#	Species	CB_Hulu calendar age (yr BP)	Cal age \pm
1002D	2 H 6	100	102.5	13.213	13.21	CAMS-59628	bulloides	29090	126
1002E	3 H 1	125	127.5	13.25	13.25	NSRL-13116	bulloides	29195	136
1002E	3 H 1	125	127.5	13.25	13.25	UCIAMS-21705	ruber	29195	136
1002D	2 H 6	105	107.5	13.263	13.26	CAMS-56892	bulloides	29221	139
1002D	2 H 6	110	112.5	13.313	13.31	CAMS-59629	bulloides	29346	154
1002E	3 H 1	135	137.5	13.34	13.34	NSRL-13117	bulloides	29419	163
1002D	2 H 6	115	117.5	13.363	13.36	CAMS-56893	bulloides	29466	170
1002D	2 H 6	120	122.5	13.413	13.41	CAMS-59630	bulloides	29582	187
1002E	3 H 1	145	147.5	13.43	13.43	NSRL-13118	bulloides	29627	194
1002D	2 H 6	125	127.5	13.463	13.46	CAMS-56894	bulloides	29693	204
1002D	2 H 6	130	132.5	13.513	13.51	CAMS-52759	bulloides	29800	222
1002E	3 H 1	5	7.5	13.54	13.54	NSRL-13119	bulloides	29862	232
1002D	2 H 6	135	137.5	13.563	13.56	CAMS-59631	bulloides	29903	239
1002D	2 H 6	140	142.5	13.613	13.61	CAMS-56895	bulloides	30003	255
1002E	3 H 1	15	17.5	13.66	13.66	NSRL-13120	bulloides	30099	271
1002D	2 H 6	145	147.5	13.663	13.66	CAMS-59632	bulloides	30099	271
1002D	2 H 7	0	2.5	13.713	13.71	CAMS-56896	bulloides	30193	286
1002D	2 H 7	5	7.5	13.763	13.76	CAMS-59633	bulloides	30285	299
1002E	3 H 2	25	27.5	13.77	13.77	NSRL-13121	bulloides	30303	302
1002D	2 H 7	10	12.5	13.813	13.81	CAMS-56897	bulloides	30374	312
1002D	2 H 7	15	17.5	13.863	13.86	CAMS-59634	bulloides	30461	323
1002E	3 H 2	35	37.5	13.88	13.88	NSRL-13122	bulloides	30496	327
1002D	2 H 7	20	22.5	13.913	13.91	CAMS-56898	bulloides	30547	333
1002D	2 H 7	25	27.5	13.963	13.96	CAMS-59635	bulloides	30631	342
1002E	3 H 2	45	47.5	13.98	13.98	NSRL-13123	bulloides	30664	345
1002E	3 H 2	45	47.5	13.98	13.98	UCIAMS-21706	ruber	30664	345
1002D	2 HCC	0	2.5	13.993	13.99	CAMS-52760	bulloides	30681	347
1002E	3 H 2	55	57.5	14	14	NSRL-13124	bulloides	30697	348
1002D	2 HCC	5	7.5	14.043	14.04	CAMS-56899	bulloides	30763	354
1002E	3 H 2	65	67.5	14.065	14.07	NSRL-13125	bulloides	30812	357
1002D	2 HCC	10	12.5	14.093	14.09	CAMS-59636	bulloides	30844	359
1002E	3 H 2	75	77.5	14.1	14.1	NSRL-13126	bulloides	30861	360
1002E	3 H 2	80	82.5	14.12	14.16	UCIAMS-21707	ruber	30957	364
1002E	3 H 2	85	87.5	14.14	14.21	NSRL-13127	bulloides	31038	366
1002D	2 HCC	15	17.5	14.143	14.21	CAMS-56900	bulloides	31038	366
1002E	3 H 2	90	92.5	14.16	14.27	UCIAMS-21708	ruber	31134	367
1002E	3 H 2	95	97.5	14.18	14.33	NSRL-13128	bulloides	31231	365
1002E	3 H 2	100	102.5	14.2	14.39	UCIAMS-3461	bulloides	31329	362
1002E	3 H 2	100	102.5	14.2	14.39	UCIAMS-21709	ruber	31329	362
1002D	3 H 1	0	2.5	14.213	14.42	CAMS-59637	bulloides	31378	359
1002E	3 H 2	105	107.5	14.23	14.47	NSRL-13129	bulloides	31462	354
1002E	3 H 2	105	107.5	14.23	14.47	UCIAMS-21710	ruber	31462	354
1002E	3 H 2	110	112.5	14.26	14.56	UCIAMS-3462	bulloides	31615	340
1002E	3 H 2	110	112.5	14.26	14.56	UCIAMS-3560	bulloides	31615	340
1002E	3 H 2	110	112.5	14.26	14.56	UCIAMS-21711	ruber	31615	340
1002D	3 H 1	5	7.5	14.263	14.56	CAMS-56901	bulloides	31615	340

Cariaco ¹⁴ C age	Cariaco ¹⁴ C age (res corr)	Cariaco ¹⁴ C ±	Comments	Deleted	CB_Hulu calendar age (yr BP)	Cal age ±	Cariaco average ¹⁴ C age (420 yr res corr)	¹⁴ C ±	Cariaco avg Δ ¹⁴ C	Δ ¹⁴ C ±
24840	24420	60			54859	641	49380	2000	630	410
25600	25180	130	duplicate		55803	618	48480	1800	1044	462
25370	24950	60	duplicate		56991	562	51630	1250	595	249
24290	23870	150		X (a)	57999	470	53180	1500	485	279
25480	25060	140			59012	337	55880	1800	200	271
25550	25130	120			60007	290	53680	1600	779	357
24680	24260	150		X (a)	60917	443	50680	2550	1886	931
25460	25040	140			61806	596	55880	3500	682	756
25750	25330	100								
25520	25100	150								
26010	25590	210								
26400	25980	140								
26000	25580	170								
25610	25190	150		X (a)						
26400	25980	180								
26320	25900	180								
26600	26180	180								
27590	27170	140		X (a)						
26300	25880	140								
26850	26430	170		X (a)						
27700	27280	210		X (a)						
26300	25880	180								
26150	25730	160								
27690	27270	190		X (a)						
27300	26880	160	duplicate	X (d)						
26670	26250	80	duplicate							
26370	25950	90								
26400	25980	140								
26360	25940	180								
26900	26480	150								
26730	26310	170								
26800	26380	170								
27370	26950	70								
27600	27180	210								
26340	25920	160		X (a)						
27340	26920	110								
27500	27080	230								
28240	27820	210	duplicate							
27950	27530	80	duplicate							
23690	23270	130		X (a)						
28300	27880	230	duplicate							
28140	27720	80	duplicate							
27730	27310	210	triplicate	X (d)						
28200	27780	180	triplicate							
28320	27900	80	triplicate							
24080	23660	160		X (a)						

Table 1 (Continued)

ODP Hole	Section	Upper depth	Lower depth	Composite depth (mbsf)	Adjusted depth (mbsf)	AMS lab ID#	Species	CB_Hulu calendar age (yr BP)	Cal age \pm
1002E	3 H 2	115	117.5	14.28	14.62	NSRL-13130	bulloides	31720	329
1002E	3 H 2	120	122.5	14.295	14.67	UCIAMS-3463	bulloides	31811	318
1002D	3 H 1	10	12.5	14.303	14.67	CAMS-59638	bulloides	31811	318
1002E	3 H 2	125	127.5	14.31	14.7	NSRL-13131	bulloides	31866	311
1002D	3 H 1	15	17.5	14.353	14.82	CAMS-56902	bulloides	32099	279
1002E	3 H 2	130	132.5	14.36	14.85	UCIAMS-3464	mixed	32160	271
1002D	3 H 1	20	22.5	14.403	14.96	CAMS-59639	bulloides	32398	240
1002E	3 H 2	135	137.5	14.41	14.97	NSRL-13132	mixed	32421	237
1002D	3 H 1	25	27.5	14.453	15.01	CAMS-56903	bulloides	32514	228
1002E	3 H 2	140	142.5	14.465	15.03	UCIAMS-2545	mixed	32561	223
1002E	3 H 2	145	147.5	14.49	15.05	NSRL-13133	mixed	32610	219
1002D	3 H 1	30	32.5	14.502	15.06	CAMS-52761	bulloides	32635	218
1002E	3 H 3	0	2.5	14.51	15.07	UCIAMS-2546	bulloides	32660	216
1002E	3 H 3	5	7.5	14.54	15.1	NSRL-13134	bulloides	32736	212
1002D	3 H 1	35	37.5	14.543	15.1	CAMS-59640	bulloides	32736	212
1002D	3 H 1	40	42.5	14.593	15.15	CAMS-56904	bulloides	32866	209
1002E	3 H 3	15	17.5	14.597	15.16	NSRL-13135	bulloides	32893	209
1002D	3 H 1	45	47.5	14.643	15.2	CAMS-59641	bulloides	33000	210
1002E	3 H 3	25	27.5	14.68	15.24	NSRL-13136	bulloides	33110	212
1002D	3 H 1	50	52.5	14.692	15.25	CAMS-56905	bulloides	33137	213
1002D	3 H 1	55	57.5	14.733	15.29	CAMS-59642	bulloides	33248	218
1002D	3 H 1	60	62.5	14.783	15.34	CAMS-56906	bulloides	33386	225
1002D	3 H 1	65	67.5	14.833	15.39	CAMS-59643	bulloides	33525	231
1002D	3 H 1	70	72.5	14.882	15.44	CAMS-56907	bulloides	33662	236
1002D	3 H 1	75	77.5	14.923	15.48	CAMS-59644	bulloides	33769	238
1002D	3 H 1	80	82.5	14.973	15.53	CAMS-52762	bulloides	33901	239
1002D	3 H 1	80	82.5	14.973	15.53	UCIAMS-21712	ruber	33901	239
1002D	3 H 1	90	92.5	15.073	15.63	UCIAMS-2525	bulloides	34153	233
1002D	3 H 1	95	97.5	15.113	15.67	UCIAMS-2526	bulloides	34250	231
1002D	3 H 1	105	107.5	15.213	15.77	NSRL-12287	bulloides	34484	230
1002D	3 H 1	115	117.5	15.303	15.86	UCIAMS-2527	mixed	34688	230
1002D	3 H 1	125	127.5	15.403	15.96	UCIAMS-2528	mixed	34908	231
1002D	3 H 1	130	132.5	15.453	16.01	CAMS-53794	bulloides	35015	232
1002D	3 H 1	135	137.5	15.498	16.06	UCIAMS-21713	ruber+bull	35120	235
1002D	3 H 1	140	142.5	15.543	16.1	UCIAMS-21717	mixed	35202	238
1002D	3 H 1	145	147.5	15.593	16.15	UCIAMS-2531	mixed	35303	243
1002D	3 H 1	145	147.5	15.593	16.15	UCIAMS-21718	mixed	35303	243
1002D	3 H 2	0	2.5	15.636	16.2	UCIAMS-21719	mixed	35400	248
1002D	3 H 2	5	7.5	15.686	16.25	NSRL-12288	mixed	35495	252
1002D	3 H 2	15	17.5	15.783	16.34	UCIAMS-2532	bulloides	35658	254
1002D	3 H 2	30	32.5	15.923	16.48	CAMS-52763	bulloides	35898	246
1002D	3 H 2	45	47.5	16.073	16.63	UCIAMS-2533	bulloides	36144	231
1002D	3 H 2	55	57.5	16.163	16.72	NSRL-12289	bulloides	36290	224
1002D	3 H 2	65	67.5	16.263	16.82	UCIAMS-2534	bulloides	36455	221
1002D	3 H 2	75	77.5	16.353	16.91	UCIAMS-2537	mixed	36607	222
1002D	3 H 2	80	82.5	16.403	16.96	CAMS-53795	bulloides	36694	225
1002D	3 H 2	85	87.5	16.453	17.01	UCIAMS-2538	mixed	36783	227
1002D	3 H 2	95	97.5	16.543	17.1	UCIAMS-2539	mixed	36946	230
1002D	3 H 2	100	102.5	16.593	17.15	UCIAMS-21720	mixed	37038	230

Cariaco ¹⁴ C age	Cariaco ¹⁴ C age (res corr)	Cariaco ¹⁴ C ±	Comments	Deleted	CB_Hulu calendar age (yr BP)	Cal age ±	Cariaco average ¹⁴ C age (420 yr res corr)	¹⁴ C ±	Cariaco avg Δ ¹⁴ C	Δ ¹⁴ C ±
28400	27980	180								
28700	28280	210								
25600	25180	110		X (a)						
28600	28180	190								
26930	26510	170		X (a)						
28480	28060	230								
26990	26570	170		X (a)						
28400	27980	180								
28500	28080	270								
29010	28590	140								
27900	27480	220								
28950	28530	110								
28710	28290	130								
28700	28280	160								
29070	28650	160								
29070	28650	110								
28900	28480	170								
28990	28570	80								
29000	28580	230								
29280	28860	110								
29390	28970	80								
29590	29170	240								
29410	28990	110								
29680	29260	110								
29690	29270	170								
29450	29030	120	duplicate							
29490	29070	90	duplicate							
29940	29520	150								
30030	29610	160								
30030	29610	210								
30530	30110	170								
30800	30380	170								
30900	30480	320								
28730	28310	130		X (d)						
30990	30570	100								
30460	30040	170	duplicate							
31190	30770	290	duplicate							
30140	29720	90		X (d)						
31750	31330	250								
31580	31160	180								
31440	31020	140								
31750	31330	180								
31880	31460	260								
32090	31670	240								
32330	31910	200								
31310	30890	290								
32530	32110	210								
32560	32140	220								
32730	32310	120								

Table 1 (Continued)

ODP Hole	Section	Upper depth	Lower depth	Composite depth (mbsf)	Adjusted depth (mbsf)	AMS lab ID#	Species	CB_Hulu calendar age (yr BP)	Cal age \pm
1002D	3 H 2	105	107.5	16.638	17.2	NSRL-12290	bulloides	37131	229
1002D	3 H 2	110	112.5	16.683	17.24	UCIAMS-3452	mixed	37206	228
1002D	3 H 2	115	117.5	16.733	17.29	UCIAMS-21721	bulloides	37301	225
1002D	3 H 2	120	122.5	16.783	17.34	UCIAMS-2540	mixed	37396	221
1002D	3 H 2	125	127.5	16.828	17.39	UCIAMS-21722	mixed	37491	215
1002D	3 H 2	130	132.5	16.873	17.43	CAMS-52764	bulloides	37568	210
1002D	3 H 2	135	137.5	16.923	17.48	UCIAMS-3455	mixed	37664	203
1002D	3 H 2	140	142.5	16.973	17.53	UCIAMS-21723	mixed	37760	196
1002D	3 H 2	145	147.5	17.023	17.58	UCIAMS-2543	mixed	37856	188
1002D	3 H 3	5	7.5	17.113	17.67	NSRL-12291	mixed	38028	174
1002D	3 H 3	10	12.5	17.163	17.72	UCIAMS-3456	mixed	38124	167
1002D	3 H 3	20	22.5	17.262	17.82	UCIAMS-2544	bulloides	38313	162
1002D	3 H 3	30	32.5	17.353	17.91	CAMS-52765	bulloides	38482	168
1002D	3 H 3	40	42.5	17.453	18.01	UCIAMS-17581	ruber	38669	183
1002D	3 H 3	40	42.5	17.453	18.01	NSRL-13085	bulloides	38669	183
1002D	3 H 3	45	47.5	17.493	18.05	UCIAMS-3457	bulloides	38744	190
1002D	3 H 3	45	47.5	17.493	18.05	UCIAMS-3559	bulloides	38744	190
1002D	3 H 3	55	57.5	17.593	18.15	NSRL-12292	bulloides	38932	210
1002D	3 H 3	60	62.5	17.643	18.2	UCIAMS-3458	bulloides	39027	220
1002D	3 H 3	70	72.5	17.733	18.29	NSRL-12293	bulloides	39199	236
1002D	3 H 3	70	72.5	17.733	18.29	UCIAMS-21724	ruber	39199	236
1002D	3 H 3	80	82.5	17.833	18.39	CAMS-52766	bulloides	39395	252
1002D	3 H 3	90	92.5	17.923	18.48	NSRL-12294	bulloides	39576	262
1002D	3 H 3	105	107.5	18.066	18.63	NSRL-12295	bulloides	39893	274
1002D	3 H 3	110	112.5	18.113	18.67	UCIAMS-16550	bulloides	39980	276
1002D	3 H 3	120	122.5	18.213	18.77	NSRL-12296	bulloides	40201	282
1002D	3 H 3	120	122.5	18.213	18.77	UCIAMS-21728	ruber	40201	282
1002D	3 H 3	125	127.5	18.263	18.82	UCIAMS-21729	bulloides	40313	284
1002D	3 H 3	130	132.5	18.303	18.86	CAMS-52767	bulloides	40403	286
1002D	3 H 3	140	142.5	18.403	18.96	NSRL-12297	bulloides	40631	289
1002D	3 H 4	0	2.5	18.497	19.06	UCIAMS-21730	bulloides	40859	290
1002D	3 H 4	5	7.5	18.543	19.1	NSRL-12298	bulloides	40950	289
1002D	3 H 4	10	12.5	18.59	19.15	UCIAMS-21731	bulloides	41064	287
1002D	3 H 4	20	22.5	18.683	19.24	NSRL-12299	bulloides	41268	278
1002D	3 H 4	30	32.5	18.783	19.34	CAMS-52768	bulloides	41492	262
1002D	3 H 4	40	42.5	18.873	19.43	UCIAMS-17582	ruber	41690	241
1002D	3 H 4	40	42.5	18.873	19.43	NSRL-13086	bulloides	41690	241
1002D	3 H 4	50	52.5	18.973	19.53	UCIAMS-16551	bulloides	41906	222
1002D	3 H 4	55	57.5	19.023	19.58	NSRL-12300	bulloides	42012	217
1002D	3 H 4	60	62.5	19.063	19.62	UCIAMS-16552	bulloides	42096	217
1002D	3 H 4	65	67.5	19.113	19.67	UCIAMS-21732	bulloides	42199	219
1002D	3 H 4	70	72.5	19.163	19.72	UCIAMS-17583	ruber	42301	223
1002D	3 H 4	70	72.5	19.163	19.72	NSRL-13087	bulloides	42301	223
1002D	3 H 4	80	82.5	19.253	19.81	CAMS-52769	bulloides	42483	227
1002D	3 H 4	90	92.5	19.353	19.91	UCIAMS-21733	bulloides	42685	225
1002D	3 H 4	105	107.5	19.493	20.05	NSRL-12301	bulloides	42977	208
1002D	3 H 4	130	132.5	19.733	20.29	CAMS-53796	bulloides	43539	155
1002D	3 H 5	5	7.5	19.973	20.53	NSRL-12302	bulloides	44228	126
1002D	3 H 5	30	32.5	20.213	20.77	CAMS-53797	bulloides	44889	175
1002D	3 H 5	55	57.5	20.443	21	NSRL-12303	bulloides	45393	231

Cariaco ¹⁴ C age	Cariaco ¹⁴ C age (res corr)	Cariaco ¹⁴ C ±	Comments	Deleted	CB_Hulu calendar age (yr BP)	Cal age ±	Cariaco average ¹⁴ C age (420 yr res corr)	¹⁴ C ±	Cariaco avg Δ ¹⁴ C	Δ ¹⁴ C ±
32640	32220	280								
33140	32720	310								
32900	32480	360								
33260	32840	220								
33310	32890	130								
33020	32600	170								
32150	31730	330		X (d)						
33260	32840	220								
33360	32940	240								
33700	33280	280								
33260	32840	320								
33810	33390	240								
33920	33500	180								
33790	33370	150	duplicate							
34400	33980	370	duplicate							
33710	33290	440	duplicate							
33910	33490	250	duplicate							
34100	33680	300								
34340	33920	420								
35010	34590	330	duplicate							
34520	34100	150	duplicate							
34620	34200	220								
34640	34220	320								
35100	34680	390								
35090	34670	150								
36000	35580	380	duplicate							
34680	34260	150	duplicate							
35020	34600	150								
35300	34880	210								
35800	35380	370								
35880	35460	160								
36400	35980	400								
36430	36010	320								
37100	36680	500								
36810	36390	260								
37240	36820	190	duplicate							
37660	37240	490	duplicate							
37960	37540	290								
38200	37780	430								
38450	38030	220								
38010	37590	390								
37030	36610	260	duplicate	X (b)						
39200	38780	520	duplicate							
38920	38500	350								
39460	39040	460								
40700	40280	680								
40490	40070	450								
41400	40980	640								
41480	41060	510								
41650	41230	650								

Table 1 (Continued)

ODP Hole	Section	Upper depth	Lower depth	Composite depth (mbsf)	Adjusted depth (mbsf)	AMS lab ID#	Species	CB_Hulu calendar age (yr BP)	Cal age ±
1002D	3 H 5	80	82.5	20.683	21.24	CAMS-53798	bulloides	45852	257
1002D	3 H 5	105	107.5	20.923	21.48	NSRL-12304	bulloides	46313	244
1002D	3 H 5	130	132.5	21.163	21.72	CAMS-53799	bulloides	46850	201
1002D	3 H 6	5	7.5	21.403	21.96	NSRL-12305	bulloides	47545	158
1002D	3 H 6	30	32.5	21.633	22.19	CAMS-53800	bulloides	48371	157
1002D	3 H 6	55	57.5	21.873	22.43	NSRL-12306	bulloides	49236	199
1002D	3 H 6	80	82.5	22.113	22.67	CAMS-53801	bulloides	49969	282
1002D	3 H 6	105	107.5	22.353	22.91	NSRL-12307	bulloides	50589	370
1002D	3 H 6	130	132.5	22.593	23.15	CAMS-56383	bulloides	51133	449
1002D	3 H 7	5	7.5	22.823	23.38	NSRL-12308	bulloides	51611	512
1002D	3 H 7	30	32.5	23.063	23.62	CAMS-56384	bulloides	52081	563
1002D	3 HCC	20	22.5	23.573	24.13	CAMS-56385	bulloides	53041	630
1002D	4 H 1	35	37.5	24.043	24.6	CAMS-56386	bulloides	53927	650
1002D	4 H 1	85	87.5	24.516	25.08	CAMS-56387	bulloides	54859	641
1002D	4 H 1	135	137.5	24.993	25.55	CAMS-56388	bulloides	55803	618
1002D	4 H 2	45	47.5	25.563	26.12	CAMS-70071	mixed	56991	562
1002D	4 H 2	45	47.5	25.563	26.12	CAMS-71099	mixed	56991	562
1002D	4 H 2	95	97.5	26.033	26.59	CAMS-70072	mixed	57999	470
1002D	4 H 2	95	97.5	26.033	26.59	CAMS-71100	mixed	57999	470
1002D	4 H 2	145	147.5	26.503	27.06	CAMS-70073	mixed	59012	337
1002D	4 H 2	145	147.5	26.503	27.06	CAMS-71101	mixed	59012	337
1002D	4 H 3	45	47.5	26.983	27.54	CAMS-70074	bulloides	60007	290
1002D	4 H 3	45	47.5	26.983	27.54	CAMS-71102	bulloides	60007	290
1002D	4 H 3	95	97.5	27.453	28.01	CAMS-70075	bulloides	60917	443
1002D	4 H 3	95	97.5	27.453	28.01	CAMS-71103	bulloides	60917	443
1002D	4 H 3	145	147.5	27.923	28.48	CAMS-70076	bulloides	61806	596
1002D	4 H 3	145	147.5	27.923	28.48	CAMS-71104	bulloides	61806	596

Cariaco ¹⁴ C age	Cariaco ¹⁴ C age (res corr)	Cariaco ¹⁴ C ±	Comments	Deleted	CB_Hulu calendar age (yr BP)	Cal age ±	Cariaco average ¹⁴ C age (420 yr res corr)	¹⁴ C ±	Cariaco avg Δ ¹⁴ C	Δ ¹⁴ C ±
44110	43690	700								
44200	43780	910								
44640	44220	740								
45700	45280	1100								
46340	45920	920								
46900	46480	1270								
47500	47080	1100								
47500	47080	1180								
47400	46980	1500								
49200	48780	1720								
47000	46580	1400								
49200	48780	1900								
49200	48780	1900								
49800	49380	2000								
48900	48480	1800								
51600	51180	1300	duplicate							
52500	52080	1200	duplicate							
53000	52580	1600	duplicate							
54200	53780	1400	duplicate							
47460	47040	810	duplicate	X (d)						
56300	55880	1800	duplicate							
54000	53580	1800	duplicate							
54200	53780	1400	duplicate							
51900	51480	2600	duplicate							
50300	49880	2500	duplicate							
56100	55680	2300	duplicate							
56500	56080	4700	duplicate							

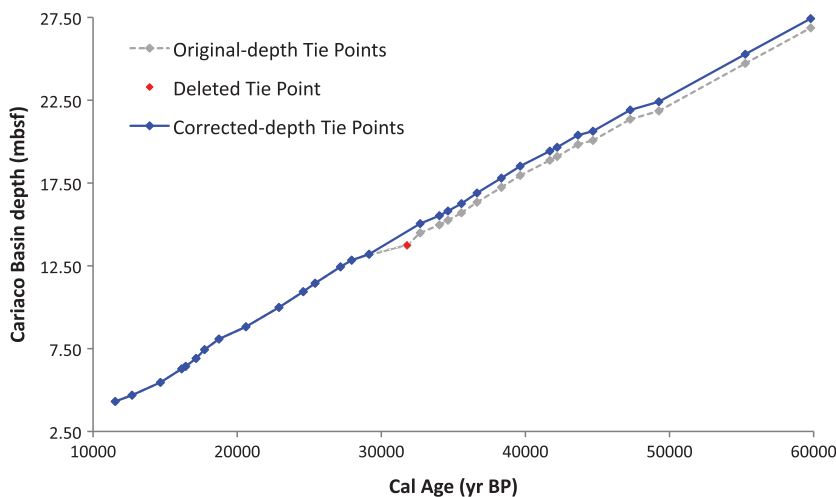


Figure 4 Cariaco-Hulu age-depth models shown over the entire time scale. The revised age-depth curve (blue) is smoother overall and shows fewer abrupt changes than previously (gray).

curve; and/or that an assumption of constant MRA/DCF depletion over time is not appropriate.

Both systems sample atmospheric ^{14}C indirectly. The world's ocean sequesters ^{14}C away from replenishment at the surface long enough for significant decay to occur, and thus surface waters appear older than the contemporary atmosphere with a global average, present day, MRA of ~ 400 years, although with substantial spatial variability (Reimer and Reimer 2001). The Cariaco Basin MRA has been measured in recent, pre-bomb sediments of known calendar age (Hughen et al. 1996), and by comparison with overlapping tree rings (Kromer and Spurk 1998; Kromer et al. 2004) further back in time during Deglaciation, to yield a value of 420 ± 50 ^{14}C yrs (Hughen et al. 2000). Speleothems also exhibit ^{14}C depletion as groundwater feeding Hulu Cave filters through overlying soil and bedrock, absorbing “ ^{14}C -dead” CO_2 and giving the growing speleothems a DCF equivalent to $\sim 450 \pm 70$ ^{14}C yrs (Southon et al. 2012).

Over the period from 11–14 cal kyr BP, it is possible to obtain an estimate of MRA within the Cariaco Basin that is independent of tuning using the varved section of the record (Hughen et al. 2000). This section of the Cariaco record, with its varve-counting chronology, can be compared with radiocarbon measurements from Northern Hemisphere (NH) tree-rings taken from the IntCal20 database (Reimer et al. 2020 in this issue) that provide a direct record of atmospheric radiocarbon. Consequently, this estimate is also independent of the Hulu Cave's DCF. In Figure 7 we plot the resultant MRA estimate, obtained via a Bayesian spline. As we see, the MRA is relatively constant despite past abrupt climatic changes, such as the end of the Younger Dryas (YD) cold event around 11.5 cal kyr BP, but shows a very clear reduction in MRA during the onset of the YD around 12.8 cal kyr BP where it drops by several hundred years to near zero. For the Hulu cave speleothem, an analogous comparison to NH atmospheric trees indicates that the DCF with Hulu has remained highly constant (see Figure 6 in Heaton et al. 2020b in this issue) over the entire 11–14 cal kyr BP period.

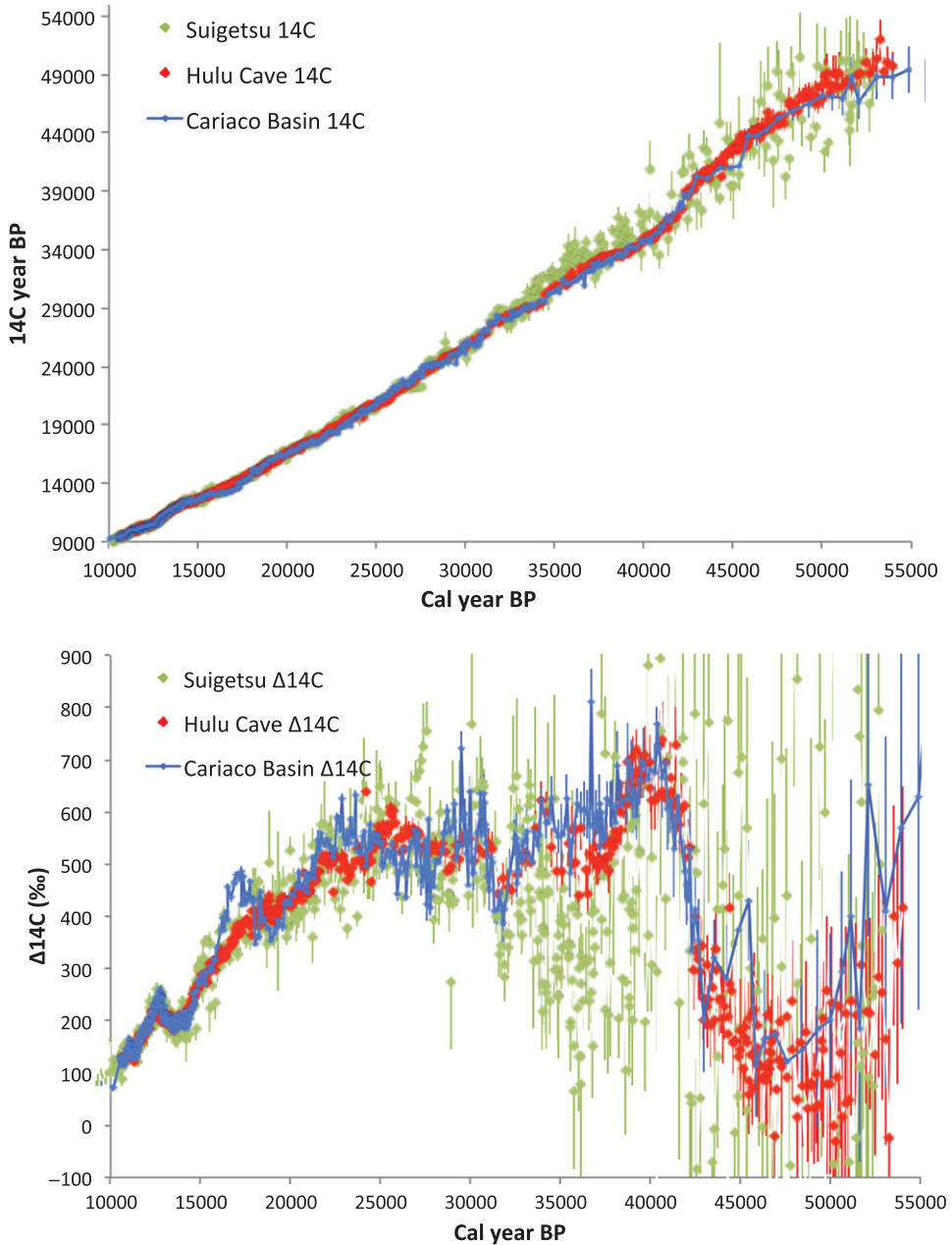


Figure 5 ^{14}C calibration dataset from the Cariaco Basin (blue) plotted versus Hulu Cave (red) and Lake Suigetsu (green) datasets. (upper) Datasets shown as age-age plots. (lower) Data plotted as original ^{14}C concentration ($\Delta^{14}\text{C}$), following corrections for calendar age decay and fractionation. The datasets show fairly close agreement from ~ 32 – 10 cal kyr BP, but increased scatter prior to that time. All ^{14}C uncertainties plotted as 1σ and include estimated uncertainties in MRA and DCF for Cariaco Basin and Hulu Cave, respectively.

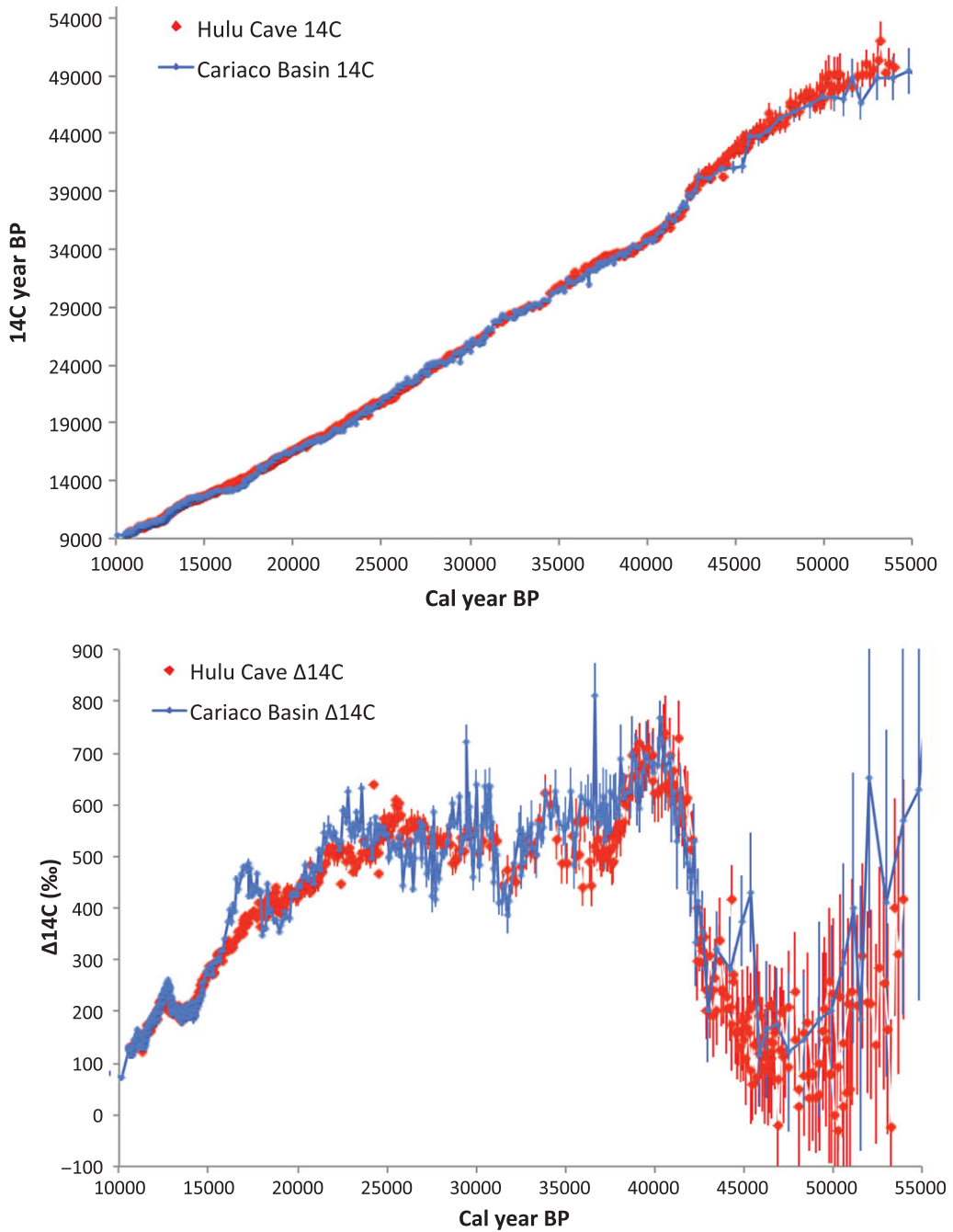


Figure 6 Same as for Figure 5, except Cariaco dataset (blue) is plotted versus Hulu Cave dataset alone (red). The close agreement between datasets is more apparent throughout the length of the records.

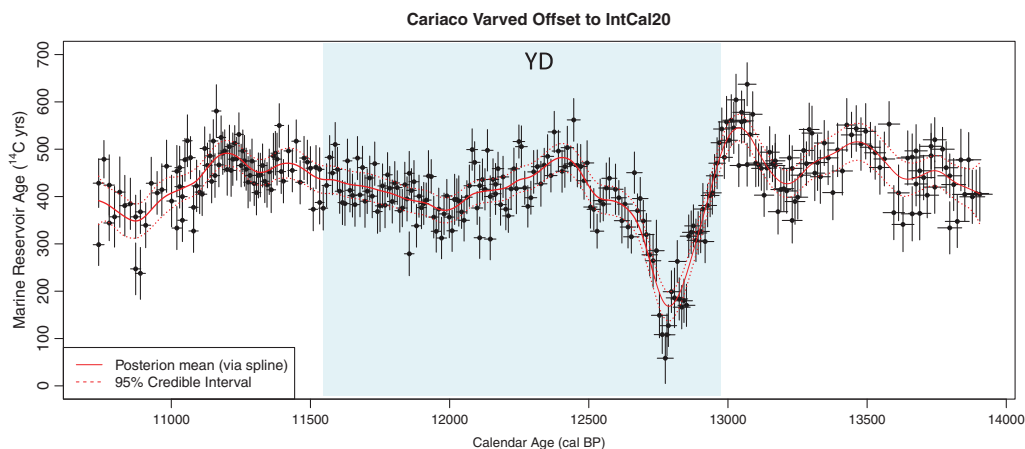


Figure 7 Cariaco MRA estimate obtained via a Bayesian spline when comparing the varved section of the record from 11–14 cal kyr BP to atmospheric tree-ring data from the IntCal20 database. The MRA estimate we obtain over this period is independent from both tuning and Hulu Cave's DCF. Each plotted point corresponds to the observed offset between an individual ^{14}C determination from the Cariaco varved record and the IntCal20 curve, which in this period is based only on tree-ring samples. The observed offsets are shown with 1σ uncertainties representing the calendar age uncertainty of the varved Cariaco ^{14}C determinations, and 1σ uncertainties in ^{14}C which incorporate both the uncertainty in the Cariaco ^{14}C sample and the IntCal20 curve at that calendar age. The MRA is relatively constant across the abrupt climate change at the YD termination (~ 11.5 cal kyr BP) but shows a clear reduction to near zero during the YD onset (~ 12.8 cal kyr BP).

The above independent comparisons of the varved Cariaco and Hulu records against NH tree-rings that provide direct sampling of atmospheric ^{14}C suggest that the periodic (and short lived) offsets between Hulu and the tuned Cariaco are likely due to MRA changes as opposed to mistuning.

Incorporating Cariaco Basin into the IntCal20 Curve

To incorporate the Cariaco Basin ^{14}C dataset into the IntCal20 curve, we need to model its MRA changes over time. For the other marine datasets used for the estimation of IntCal20, such MRA estimates were obtained using the three-dimensional Large Scale Geostrophic Ocean General Circulation Model (LSG OGCM) (Butzin et al. 2017, 2020 in this issue). However, this model does not have the resolution to simulate the unique topography of the Cariaco Basin, as evidenced by its inability to recreate the reduction in MRA seen around 12.8 cal kyr BP in Figure 7.

Consequently, we adopt a different approach to MRA modeling for the Cariaco Basin. We consider the Cariaco MRA as an unknown ^{14}C offset, via an additional Bayesian spline, and seek to adaptively estimate its value during curve construction itself based upon comparison to the other datasets¹. At each iterative step of our Markov Chain Monte Carlo curve construction approach (Heaton et al. 2020a in this issue) we update both our

¹For completeness, as for all the marine datasets, when incorporating the Cariaco samples into IntCal20 we further add an independent ^{14}C uncertainty to each ^{14}C determination to account for any additional short-term uncertainty not represented by our chosen MRA model. The size of this additional MRA variability is dataset dependent and based upon the increase needed to make that specific marine dataset consistent with the independent atmospheric NH tree-ring determinations in the 11–14 cal kyr BP time period. See Heaton et al. (2020 in this issue) for more detail.

estimate for the atmospheric ^{14}C calibration curve and our estimate for the Cariaco MRA based upon its observed offset from that curve.

This adaptive approach does introduce some questions regarding identifiability of ^{14}C changes within the Cariaco Basin record—to what extent is a feature seen within the Cariaco record due to a change in MRA within the basin, and to what extent an atmospheric event? Typically, through our chosen approach, we would expect features only seen within the Cariaco Basin to be considered a basin-specific MRA effect; while those additionally seen in other records would be considered atmospheric and reproduced in our atmospheric IntCal20 estimate.

As such, the Cariaco Basin plays a somewhat unique role in the construction of the IntCal20 curve. The additional flexibility provided by our adaptive modeling of the MRA will hopefully resolve the periods of systematic offsets between the Cariaco Basin and Hulu datasets (as seen in Figures 5 and 6) that may be due to short term MRA changes. However, the inclusion of Cariaco Basin still provides us with a better ability to recognize and retain shared features seen across multiple records and hence provide a more robust atmospheric ^{14}C curve—the intended aim of the IntCal project.

Inferred MRA Changes within Cariaco Basin over Time

As a consequence of this adaptive approach to modeling Cariaco Basin's MRA, alongside construction of the IntCal20 curve, we simultaneously obtain a posterior estimate of the MRA within the Cariaco Basin over time. This is shown in Figure 8a and is of potential independent interest. We discuss this posterior estimate below, illustrating the changing offset in the Cariaco Basin compared to Hulu cave. In building the IntCal20 (Reimer et al. 2020 in this issue) and Marine20 (Heaton et al. 2020b in this issue) curves, marine datasets were corrected for changes in MRA through time. Global MRAs were calculated using an ocean GCM (OGCM) (Butzin et al. 2020 in this issue) and applied to individual datasets according to region. However, the modeled MRA variability for the Cariaco Basin appears much too high (Figure 8b), possibly due the OGCM's inability to capture the unique bathymetry and hydrographic setting of the basin. We therefore use the posterior estimate of the MRA to correct the Cariaco ^{14}C calibration curve back through time (Heaton et al. 2020 in this issue). Due to the density of Hulu Cave measurements in the combined IntCal20 database, and the assumption of an approximately constant DCF over time within each Hulu speleothem in IntCal20 construction, this ^{14}C offset between the Cariaco and Hulu data is the primary driver for the obtained MRA estimate.

Looking closely at both our posterior MRA estimate and the apparent deviations between Cariaco Basin and Hulu Cave ^{14}C through time, we can evaluate the timing of ^{14}C change relative to rapid climate shifts in the paleoclimate record. As discussed above in Figure 7 comparing against trees that directly sample the atmosphere, the YD onset is clearly seen to coincide with an apparent reduction of Cariaco MRA by several hundred years. This is also seen when the Cariaco data is compared against the Hulu data alone (Figure 9). Similarly, Cariaco MRA appears to drop by several hundred years during the time of Heinrich Event 1 (Figure 10). The MRA decrease follows event H1b and persists throughout the transition into event H1a. However, there is no apparent change in MRA during the climatically more severe H1a event (Figure 10). The calendar age of this MRA decrease is bracketed by tie points at the end of H1b and the onset of H1a (17,148 and 16,150 cal yr BP, respectively), and falls within the older half of an anomalous “grey layer” that bears evidence of increased freshwater input and fluvial runoff (Yurco 2010).

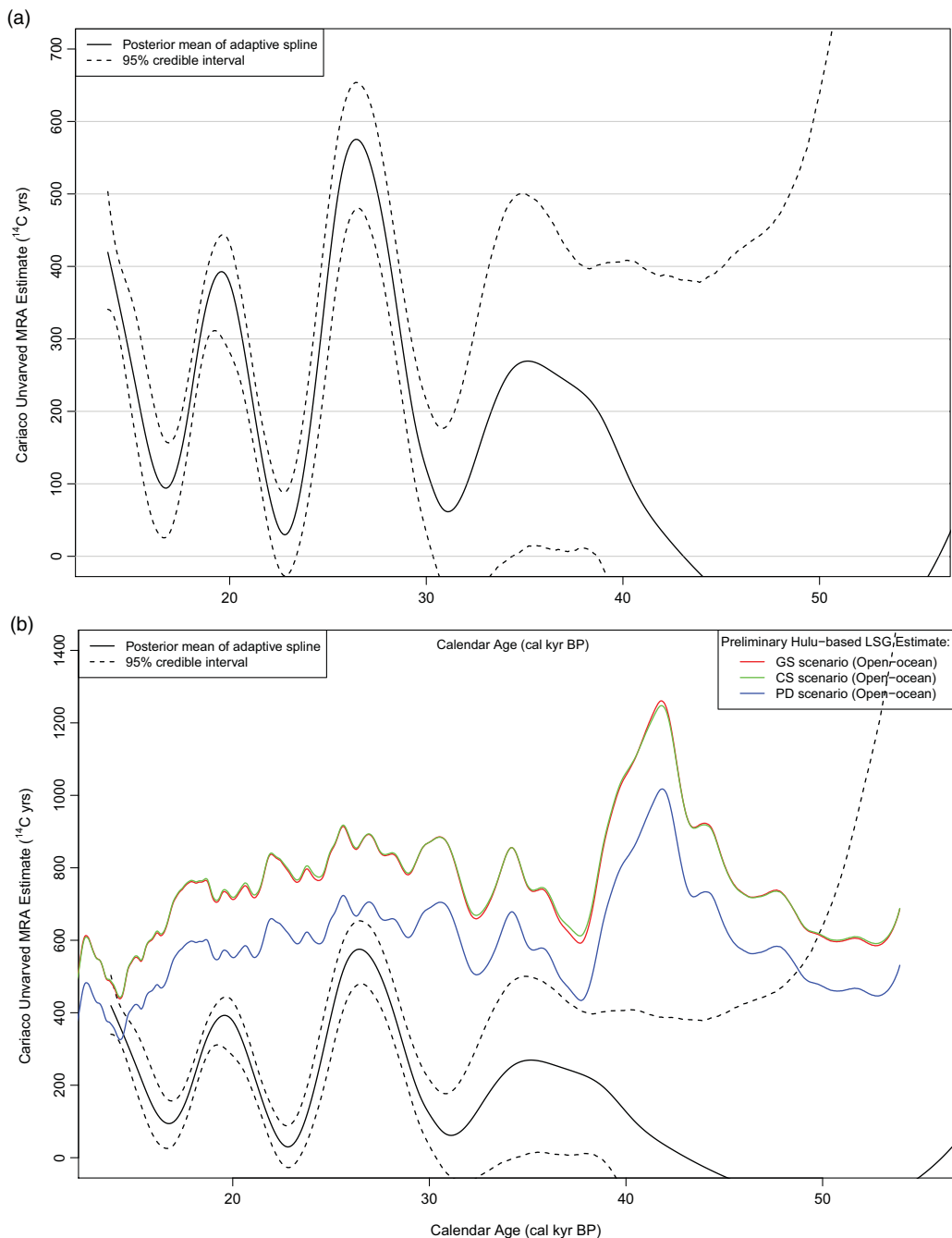


Figure 8 (a) Posterior mean estimate (shown in black with the 95% credible interval) of Cariaco Basin's MRA through time, obtained simultaneously to IntCal20 curve construction. This MRA estimate is obtained adaptively as an additive Bayesian spline at the same time as the IntCal20 curve is constructed based upon the observed offset between Cariaco and other individual ^{14}C calibration datasets used in IntCal20. The procedure captures the same timing, direction and relative magnitude of Cariaco MRA changes as seen in direct comparisons with Hulu Cave data (following figures), likely due to the density of Hulu Cave measurements in the combined IntCal20 datasets and the assumption of constant DCF depletion. (b) Cariaco posterior mean MRA estimate shown together with the estimates for the nearest open-ocean site to the Cariaco Basin obtained by the LSG OGCM under three different climate scenarios when driven by a preliminary estimate of atmospheric $\Delta^{14}\text{C}$ obtained from the Hulu cave speleothems alone (Butzin et al. 2020 in this issue). Regional first-order Hulu-based LSG OGCM estimates were used to incorporate the other marine datasets into IntCal20 (Reimer et al. 2020 in this issue) but do not appear appropriate for the Cariaco Basin, as they overestimate the variability and magnitude of MRA values through time.

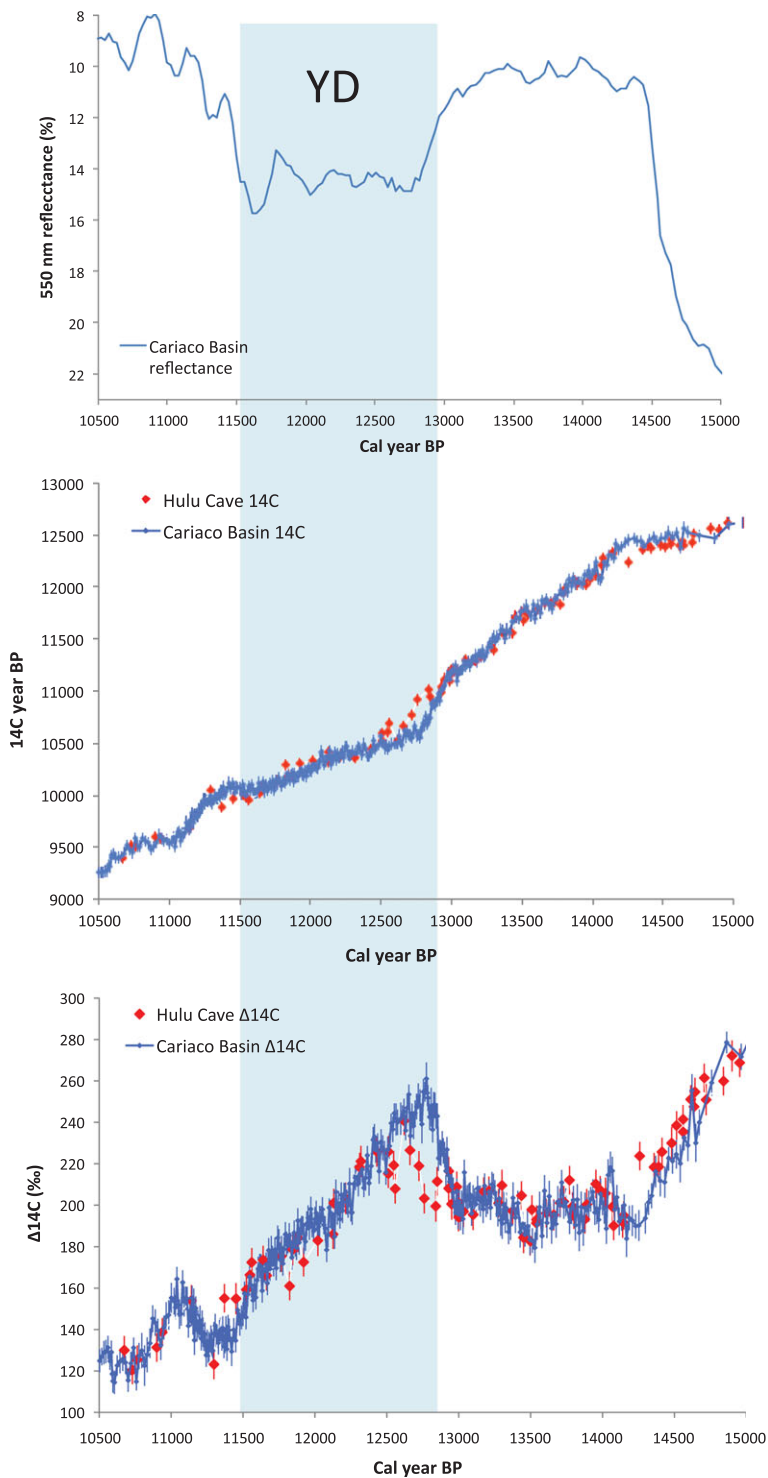


Figure 9 Detailed comparison of timing between Cariaco Basin paleoclimate and ^{14}C excursions relative to Hulu Cave (considered here as changes in MRA), focusing on the period of the Younger Dryas cold event. (upper) 550 nm reflectance from Cariaco sediments, showing periods of greater windiness (down) and greater rainfall (up). (middle) Cariaco Basin (blue) versus Hulu Cave (red) age-age plots. (lower) Cariaco Basin (blue) versus Hulu Cave (red) $\Delta^{14}\text{C}$ plots. Reduced Cariaco MRA appears as lower ^{14}C ages but higher $\Delta^{14}\text{C}$. Cariaco data are corrected with a constant 420 ± 50 ^{14}C yrs MRA (Hughen et al. 2000), and Hulu data have a constant DCF correction of 450 ± 70 ^{14}C yrs (Southon et al. 2012). These uncertainties are propagated into the plotted error bars.

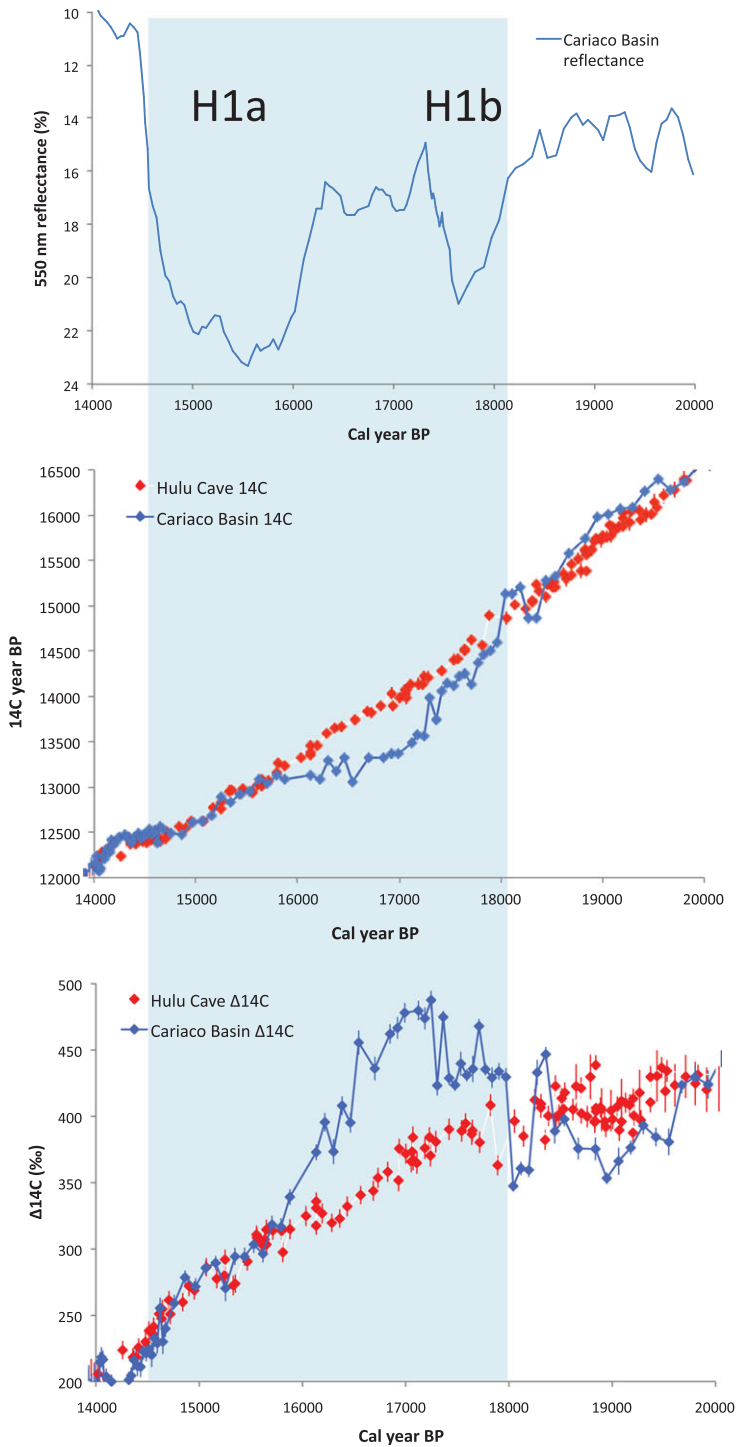


Figure 10 Same as for Figure 9 but focusing on the period surrounding Heinrich Event 1.

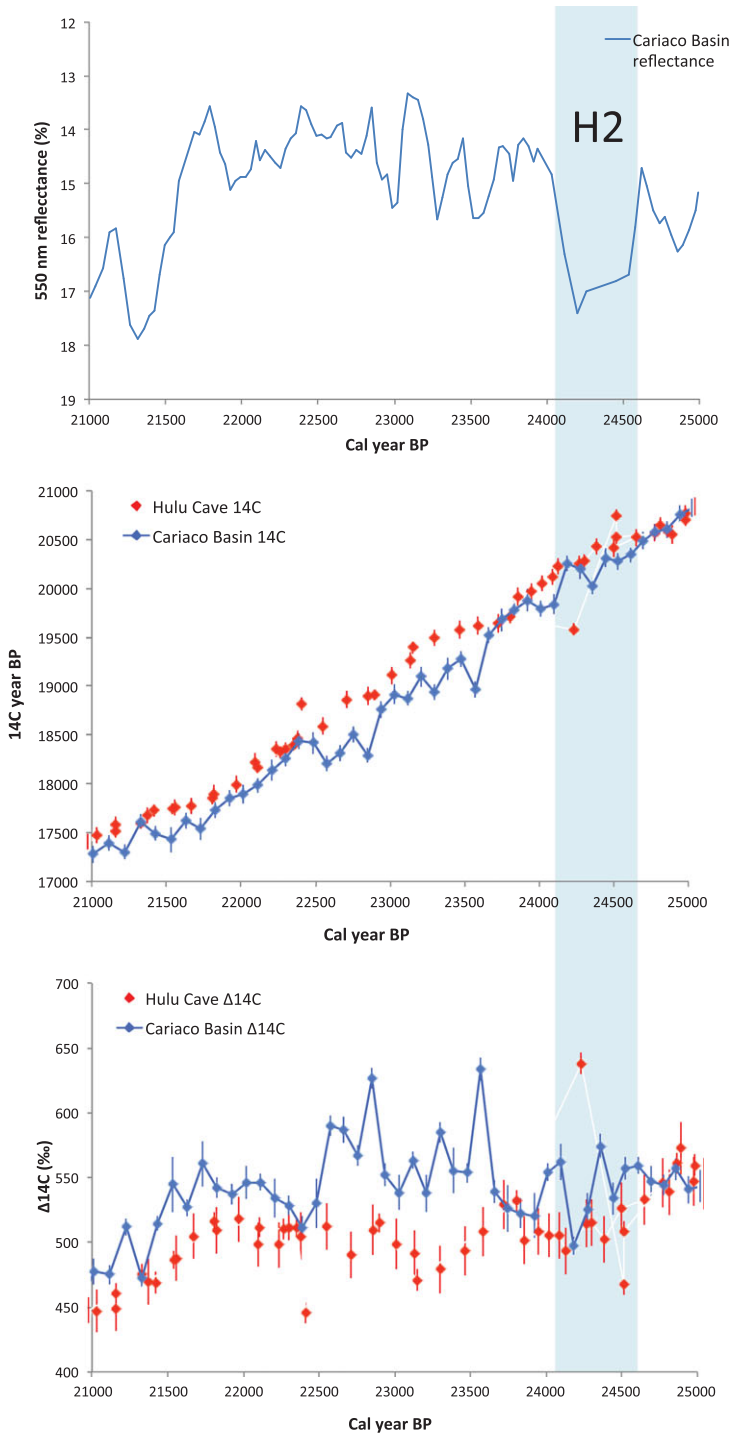


Figure 11 Same as for Figures 9 and 10 but focusing on the period surrounding Heinrich Event 2.

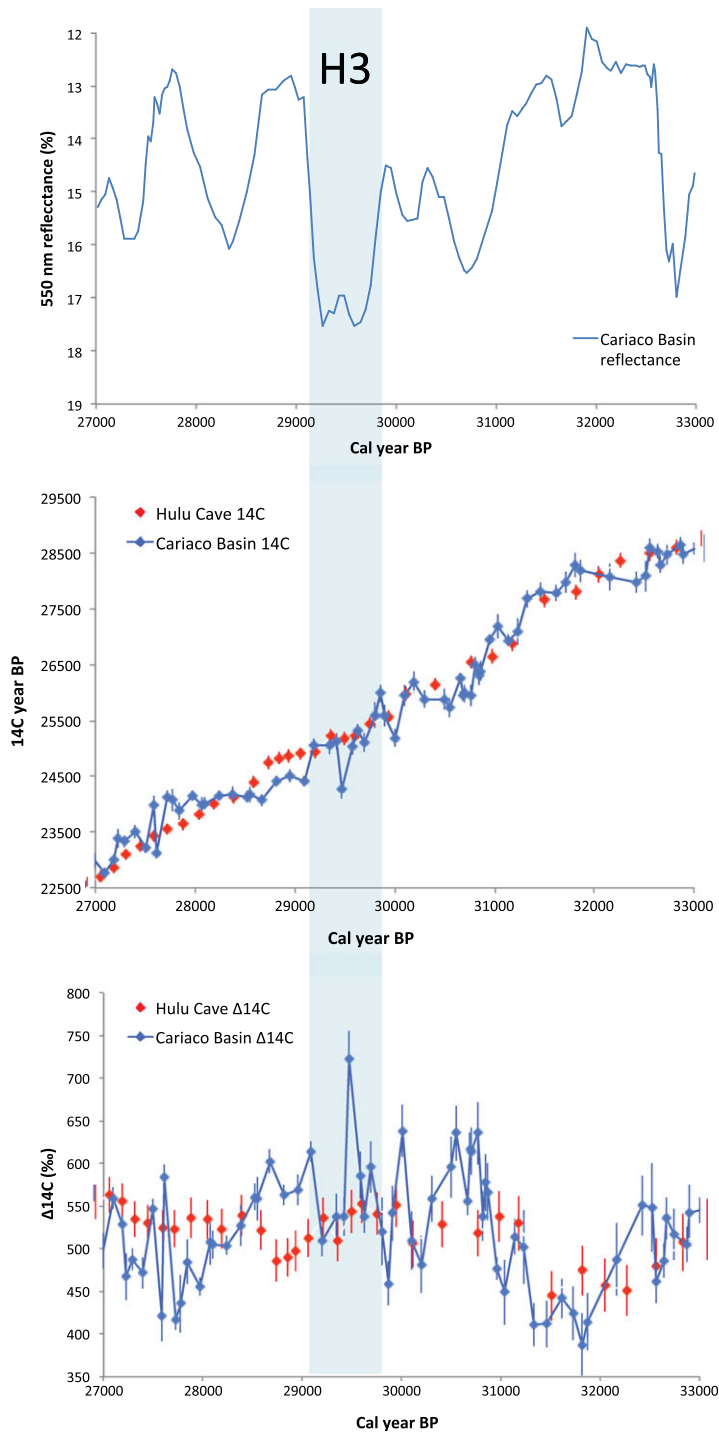


Figure 12 Same as for Figures 9–11 but focusing on the period surrounding Heinrich Event 3.

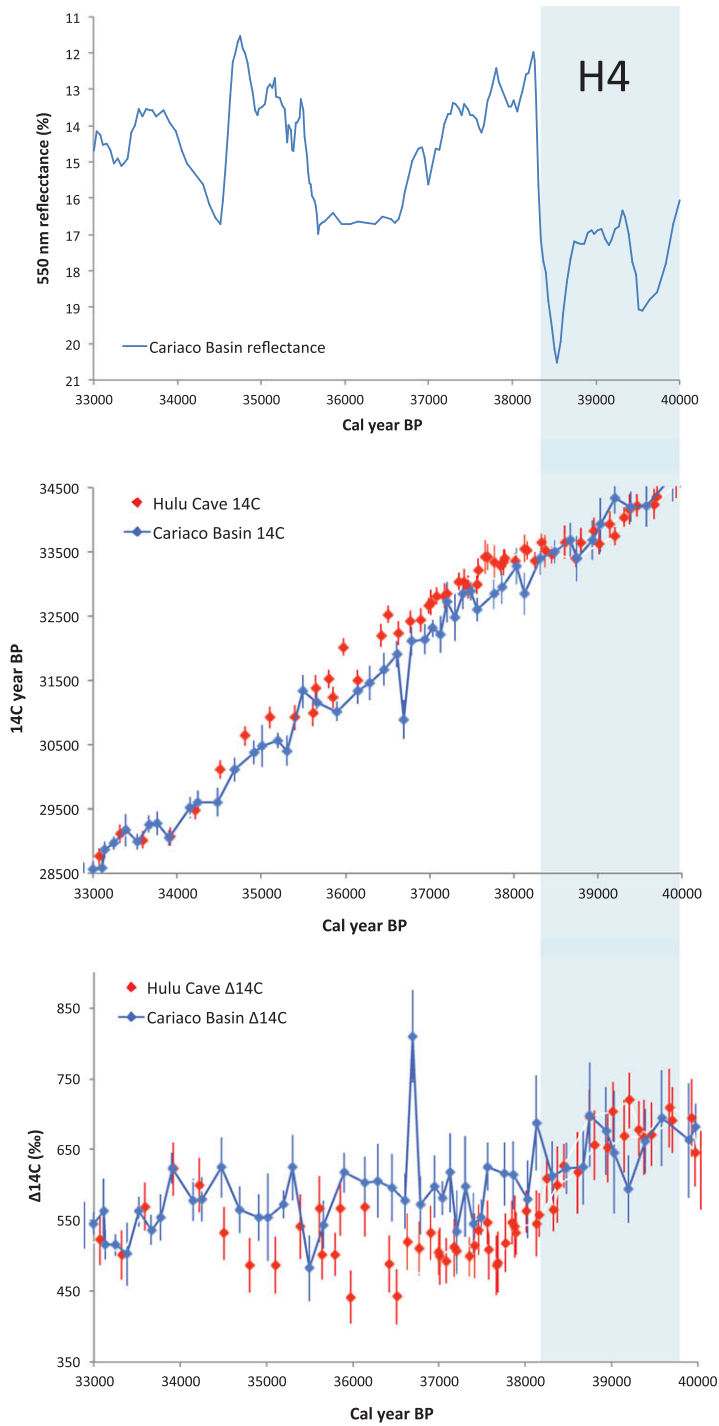


Figure 13 Same as for Figures 9–12 but focusing on the period following Heinrich Event 4.

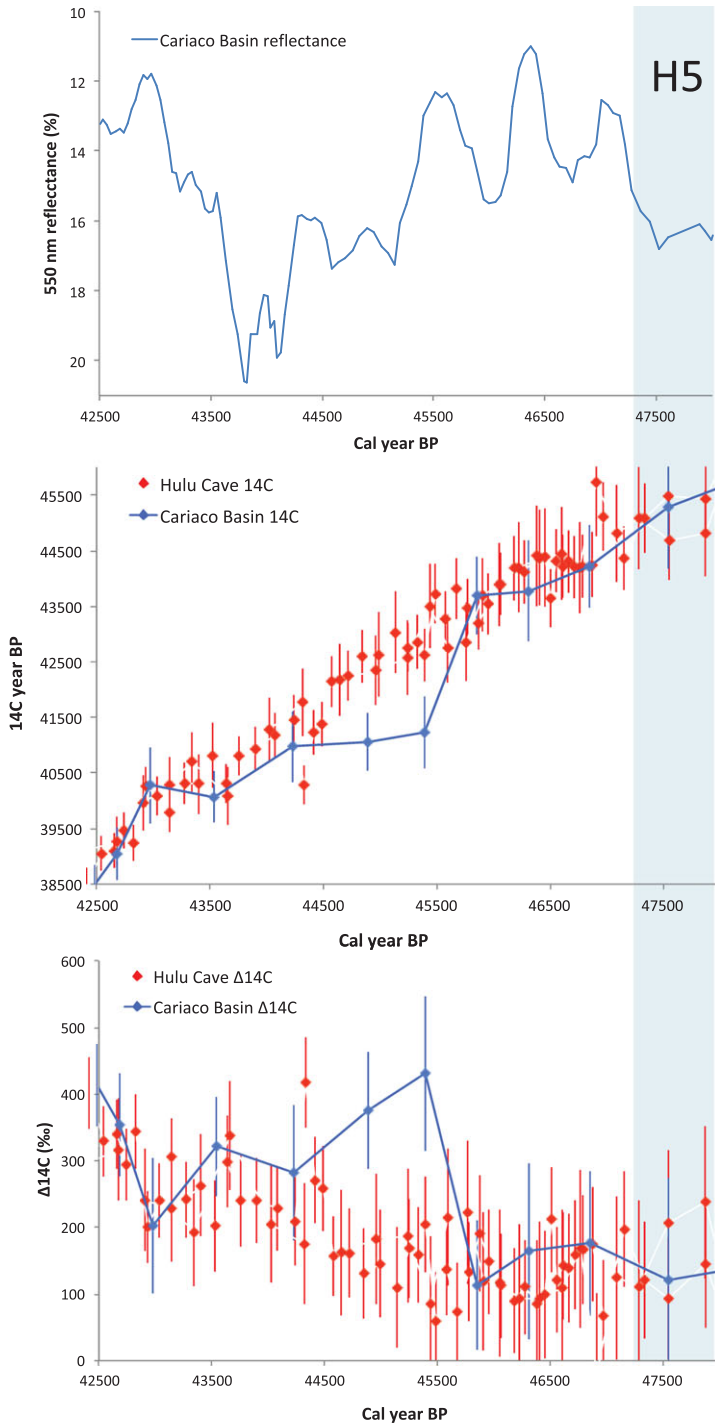


Figure 14 Same as for Figures 9–13 but focusing on the period following Heinrich Event 5.

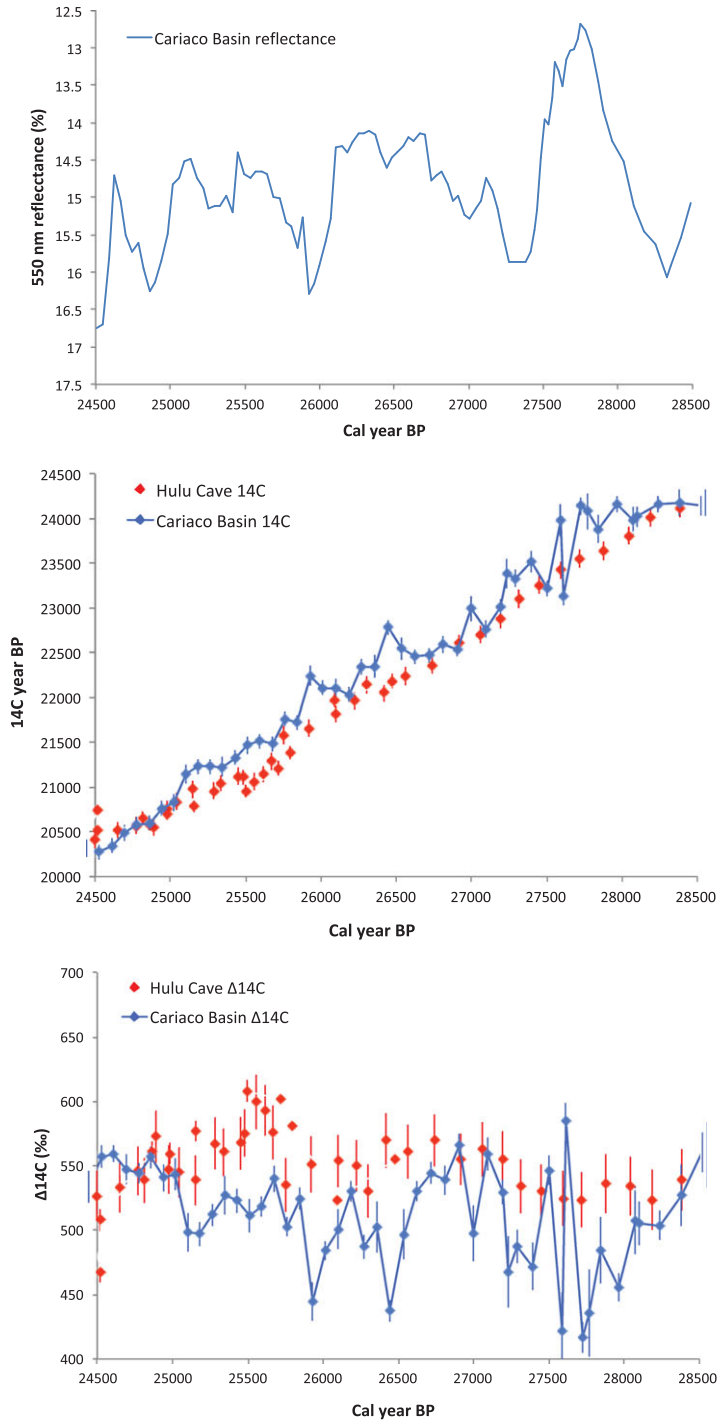


Figure 15 Same as for Figures 9–14, but focusing on a period between Heinrich Events, but characterized by increased Cariaco MRA (reduced $\Delta^{14}\text{C}$).

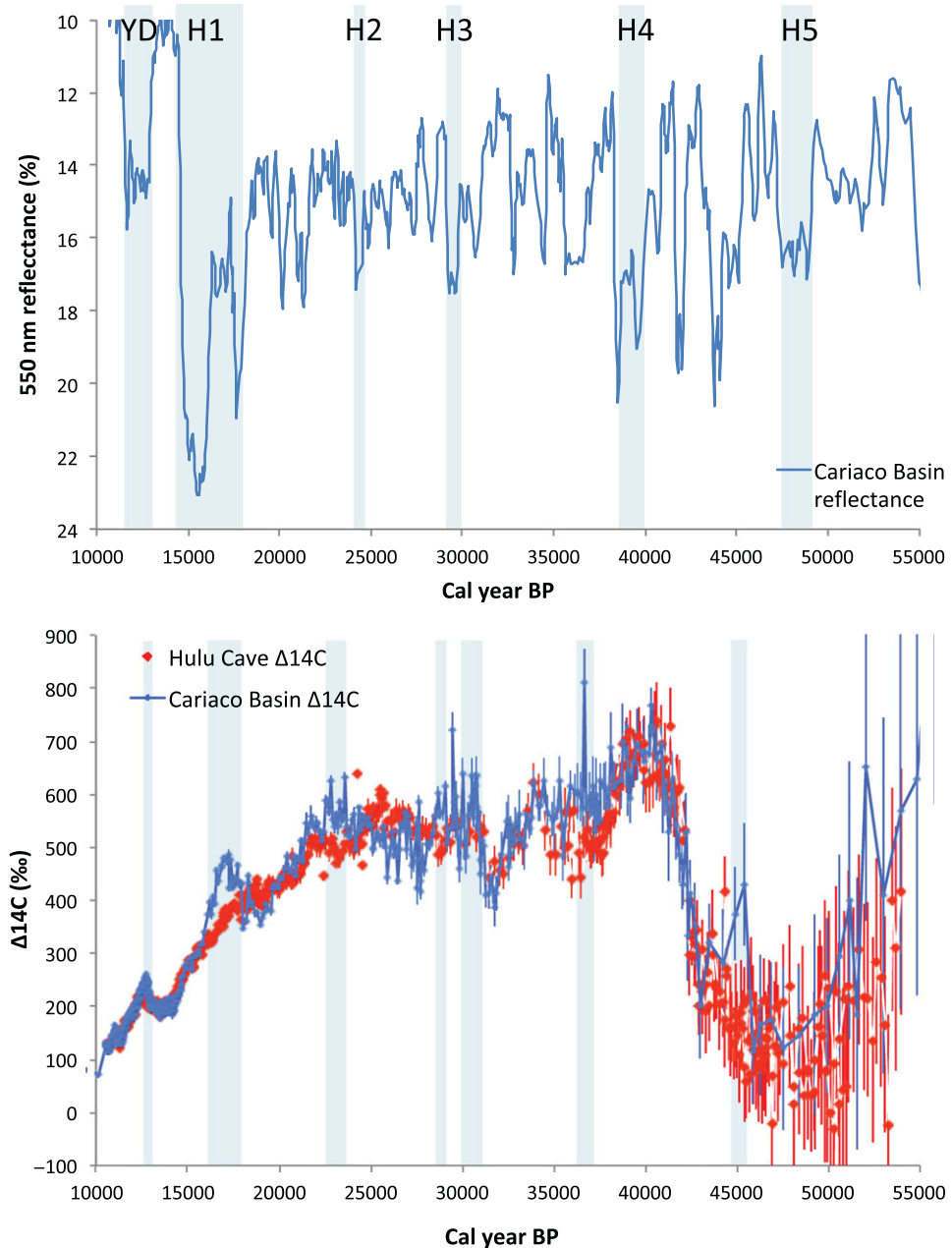


Figure 16 Comparison of timing between Cariaco Basin paleoclimate and ^{14}C excursions relative to Hulu Cave, shown over entire timescale of the data sets: (upper) 550 nm reflectance from Cariaco sediments, showing periods of greater windiness (down) and greater rainfall (up). The general timing of Heinrich Events in the Cariaco record is shown by light blue bars. (lower) Cariaco Basin (blue) versus Hulu Cave (red) $\Delta^{14}\text{C}$ plots. Periods of reduced Cariaco MRA occur every 6–7 cal kyrs (indicated by light blue bars) but appear distinct from Heinrich Events.

However, in order to explain the Cariaco ^{14}C age plateau as resulting from rapidly increased sedimentation (from terrestrial runoff), ~ 63 cm of sediment would have had to be deposited nearly instantaneously soon after event H1b. In the absence of evidence for such an extreme sedimentation event, this MRA decrease around the time of H1 appears real. Although the precise calendar age of this feature has relatively high uncertainties from the tuning process, the relative timing of the MRA decrease well before the climatic H1a stadial suggests that increased atmospheric $\Delta^{14}\text{C}$ associated with reduced AMOC (e.g., Hughen et al. 1998) may not have played a role here. Rather, the apparent reduction in Cariaco MRA is likely associated with decreased mixing of deep waters due to increased stratification in surface waters of the tropical North Atlantic or Cariaco Basin region.

The general timing of periods of reduced Cariaco MRAs reveals that an episode occurred approximately every 6–7 cal kyrs, suggestive of the intervals between Heinrich Events (Rasmussen et al. 2014). To test for a potential link between climate and MRA changes, we examine the detailed evidence for reduced Cariaco MRA during earlier Heinrich events (Figures 11–14). Although we do in fact observe reduced Cariaco MRA near the occurrence of Heinrich Events, the timing in general is off, with reduced MRA beginning up to 2000 cal yrs after the onset of the climatic events (Figures 11–14). In addition to reduced MRA, we also see evidence for a period of increased MRA between 28 and 25 cal kyr BP (Figure 15). Although there was likely an overall increase in MRA during the Glacial period, due to reduced carbon reservoirs in the atmosphere, biosphere and shallow ocean sediments (e.g., Hughen et al. 2004a), this would not explain a short interval of increased MRA from 25–28 cal kyr BP. This interval instead appears to be part of the cyclical pattern of Cariaco MRA changes (Figure 8a) and may represent a period of relatively weak stratification and strong deep mixing (upwelling).

We note that, due to potential variability in both Hulu DCF and Cariaco MRA through time, the magnitude and even exact timing of changes in the Cariaco Basin MRA cannot be determined with precision. In particular, our current estimates are heavily based upon the assumption that the DCF within Hulu Cave remained approximately constant from 0–55 cal kyr BP. If global MRA were adjusted upward due to Glacial boundary conditions, it would increase the apparent magnitude of periodic Cariaco MRA reductions, and even slightly broaden the durations of the events. Regardless, the general pattern of quasi-periodic cycles of MRA variability appears to be robust (Figures 8, 16). Overall, the disagreement in relative timing between reduced MRA in the Cariaco Basin and Heinrich Events (Figure 16) precludes reduced AMOC during H events as a potential cause. The data suggest cyclic decreases in Cariaco MRA to values below 100 ^{14}C years, despite Glacial boundary conditions that should have somewhat *increased* surface ocean MRA around the globe (Hughen et al. 2004a; Butzin et al. 2020 in this issue). These low reservoir ages are an extraordinary finding without analog in the modern ocean and are difficult to reconcile with physical or geochemical models of ocean circulation. At a minimum, these results suggest periodic swings in surface stratification in the Cariaco Basin region with times of greatly reduced mixing of ^{14}C -depleted “older” water from below. However, a clearer vision of true atmospheric ^{14}C throughout the Glacial period may be necessary in order to draw a firmer conclusion. The Lake Suigetsu record provides such an atmospheric record, but the magnitude of scatter in the current dataset precludes the identification of MRA shifts, and extension of dendrochronologies such as from floating Kauri sequences (Turney et al. 2010) may be the best solution.

CONCLUSIONS

The ¹⁴C calibration data set from intermittently varved sediments of the Cariaco Basin has been substantially updated, with changes to calendar and ¹⁴C chronologies. Revising the depth scale to reflect sediment missing from a core break provided a more accurate view of age-depth changes over the length of the record. A re-evaluation of tie points between existing Cariaco and newly updated Hulu Cave paleoclimate records resulted in the removal of one anomalous tie point, and better agreement between ¹⁴C datasets. Close comparison of Cariaco and Hulu ¹⁴C data shows periodic episodes of reduced Cariaco MRA, but coeval paleoclimate records show no direct relationship with the occurrence of Heinrich Events in the high-latitude North Atlantic region. The determination of the exact magnitude and duration of MRA variability is sensitive to long-term background changes in both Cariaco MRA and Hulu Cave DCF. However, an apparently cyclic pattern of Cariaco MRA decreases, possibly driven by increased surface ocean stratification, appears to be a robust feature of the updated record. An atmospheric ¹⁴C dataset with less scatter than the Lake Suigetsu record, potentially from floating Kauri sequences, is needed to determine the precise history of MRA variability in the Cariaco Basin and elsewhere. Nevertheless, the Cariaco ¹⁴C calibration dataset presented here incorporates several improvements over previous versions and more accurately reflects changes in both marine and atmospheric ¹⁴C through time.

ACKNOWLEDGMENTS

The authors would like to thank Prof. Edouard Bard and an anonymous reviewer for helpful comments that improved the quality of the manuscript. K.A. Hughen was supported by funds from U.S. NSF grant #OCE-1657191, and by the Investment in Science Fund at WHOI. T.J. Heaton is supported by a Leverhulme Trust Fellowship RF-2019-140/9, “Improving the Measurement of Time Using Radiocarbon”.

SUPPLEMENTARY MATERIAL

To view supplementary material for this article, please visit <https://doi.org/10.1017/RDC.2020.53>

REFERENCES

- Bronk Ramsey C, Staff RA, Bryant CL, Brock F, Kitagawa H, van der Plicht J, Schlolaut G, Marshall MH, Brauer A, Lamb HF, Payne RL, Tarasov PE, Haraguchi, T, Gotanda, K, Yonenobu H, Yokoyama Y, Tada R, Nakagawa T. 2012. A complete terrestrial radiocarbon record for 11.2 to 52.8 kyr B.P. *Science* 338(6105):370–374. doi: [10.1126/science.1226660](https://doi.org/10.1126/science.1226660).
- Butzin M, Köhler P, Heaton TJ, Lohmann G. 2020. A short note on marine reservoir age simulations used in IntCal20. *Radiocarbon* 62. This issue. doi: [10.1017/RDC.2020.18](https://doi.org/10.1017/RDC.2020.18).
- Butzin M, Köhler P, Lohmann G. 2017. Marine radiocarbon reservoir age simulations for the past 50,000 years. *Geophys. Res. Letters* 44:8473–8480. doi: [10.1002/2017GL074688](https://doi.org/10.1002/2017GL074688).
- Cheng H, Edwards RL, Sinha A, Spötl C, Yi L, Chen S, Kelly M, Kathayat G, Wang X, Li X. 2016. The Asian monsoon over the past 640,000 years and ice age terminations. *Nature* 534(7609): 640.
- Cheng H, Edwards RL, Southon J, Matsumoto K, Feinberg JM, Sinha A, Zhou W, Li H, Li X, Xu Y. 2018. Atmospheric ¹⁴C/¹²C changes during the last glacial period from Hulu Cave. *Science* 362(6420):1293–1297.
- Heaton T, Bard E, Hughen K. 2013. Elastic tiepointing – transferring chronologies between records via a Gaussian process. *Radiocarbon* 55:1975–1997. doi: [10.2458/azu_js_rc.55.17777](https://doi.org/10.2458/azu_js_rc.55.17777).
- Heaton TJ, Blaauw M, Blackwell PG, Bronk Ramsey C, Reimer P, Scott EM. 2020a. The IntCal20

- approach to radiocarbon calibration curve construction: A new methodology using Bayesian splines and errors-in-variables. *Radiocarbon* 62. This issue. doi: [10.1017/RDC.2020.46](https://doi.org/10.1017/RDC.2020.46).
- Heaton TJ, Köhler P, Butzin M, Bard E, Reimer R, Austin WE, Bronk Ramsey C, Grootes PM, Hughen KA, Kromer B, Reimer PJ, Adkins J, Burke A, Cook MS, Olsen J, Skinner LC. 2020b. Marine20—the marine radiocarbon age calibration curve (0–55,000 cal BP). *Radiocarbon* 62. This issue. doi: [10.1017/RDC.2020.68](https://doi.org/10.1017/RDC.2020.68).
- Hogg AG, Heaton TJ, Hua Q, Palmer JG, Turney CSM, Southon J, Bayliss A, Blackwell PG, Boswijk G, Bronk Ramsey C, Pearson C, Petchey F, Reimer P, Reimer R, Wacker L. 2020. SHCal20 Southern Hemisphere calibration, 0–55,000 years cal BP. *Radiocarbon* 62. This issue. doi: [10.1017/RDC.2020.59](https://doi.org/10.1017/RDC.2020.59).
- Hughen KA, Overpeck JT, Peterson LC, Trumbore S. 1996. Rapid climate changes in the tropical Atlantic region during the last deglaciation. *Nature* 380:51–54.
- Hughen KA, Overpeck JT, Lehman SJ, Kashgarian M, Southon J, Peterson LC, Alley R, Sigman DM. 1998. Deglacial changes in ocean circulation from an extended radiocarbon calibration. *Nature* 391:65–68.
- Hughen KA, Southon JR, Lehman SJ, Overpeck JT. 2000. Synchronous radiocarbon and climate shifts during the last deglaciation. *Science* 290:1951–1954.
- Hughen KA, Lehman SJ, Southon J, Overpeck JT, Marchal O, Herring C, Turnbull J. 2004a. ^{14}C activity and global carbon cycle changes over the past 50,000 years. *Science* 303:202–207.
- Hughen KA, Baillie MGL, Bard E, Warren Beck J, Bertrand CJH, Blackwell PG, Buck CE, Burr GS, Cutler KB, Damon PE, et al. 2004b. *Radiocarbon* 46:1059–1086.
- Hughen KA, Eglinton TI, Xu L, Makou M. 2004c. Abrupt tropical vegetation response to rapid climate changes. *Science* 304:1955–1959.
- Hughen KA, Southon JA, Lehman SJ, Bertrand CJH, Turnbull J. 2006. Marine-derived ^{14}C calibration and activity record for the past 50,000 years updated from the Cariaco Basin. *Quaternary Science Reviews* 25:3216–3227.
- Johnsen S, Clausen H, Dansgaard W, et al. 1992. Irregular glacial interstadials recorded in a new Greenland ice core. *Nature* 359:311–313. doi: [10.1038/359311a0](https://doi.org/10.1038/359311a0).
- Kromer B, Spurk M. 1998. Revision and tentative extension of the tree-ring based ^{14}C calibration, 9200–11,855 cal BP. *Radiocarbon* 40:1117–1125.
- Kromer B, Friedrich M, Hughen KA, Kaiser KF, Remmele S, Schaub M, Talamo S. 2004. Late Glacial ^{14}C ages from a floating 1270-ring pine chronology. *Radiocarbon* 46:1203–1210.
- Laj C, Kissel C, Mazaud A, Michel E, Muscheler R, Beer J. 2002. Geomagnetic field intensity, North Atlantic deep water circulation and atmospheric $\Delta^{14}\text{C}$ during the last 50 kyr. *Earth and Planetary Science Letters* 200:179–192.
- Manabe S, Stouffer RJ. 1997. Coupled ocean-atmosphere model responses to freshwater input: Comparison to Younger Dryas event. *Paleoceanography* 12:321–336.
- Meese DA, Gow AJ, Alley RB, Zielinski GA, Grootes PM, Ram M, Taylor KC, Mayewski PA, Bolzan JF. 1997. The Greenland Ice Sheet Project 2 depth-age scale: Methods and results. *Journal of Geophysical Research* 102. doi: [10.1029/97JC00269](https://doi.org/10.1029/97JC00269).
- Peterson LC, Haug GH, Hughen KA, Röhl U. 2000. Rapid changes in the hydrologic cycle of the tropical Atlantic during the Last Glacial. *Science* 290:1947–1951.
- Rasmussen S, Bigler M, Blockley S, Blunier T, Buchardt SL, Clausen H, Cvijanovic I, Dahl-Jensen D, Johnsen S, Fischer H, Gkinis V, Guillevic M, Hoek WZ, Lowe J, Pedro J, Popp T, Seierstad I, Steffensen J, Svensson A, Winstrup M. 2014. A stratigraphic framework for abrupt climatic changes during the Last Glacial period based on three synchronized Greenland ice-core records: Refining and extending the INTIMATE event stratigraphy. *Quaternary Science Reviews* 106. doi: [10.1016/j.quascirev.2014.09.007](https://doi.org/10.1016/j.quascirev.2014.09.007).
- Reimer PJ, Reimer RW. 2001. A marine reservoir correction database and on-line interface. *Radiocarbon* 43:461–463.
- Reimer PJ, Baillie MGL, Bard E, Bayliss A, Beck JW, Bertrand CJH, Blackwell PG, Buck CE, Burr GS, Cutler KB, Damon PE, Edwards RL, Fairbanks RG, Friedrich M, Guilderson TP, Hogg AG, Hughen KA, Kromer B, McCormac G, Manning S, Bronk Ramsey C, Reimer RW, Remmele S, Southon JR, Stuiver M, Talamo S, Taylor FW, van der Plicht J, Weyhenmeyer CE. 2004. IntCal04 terrestrial radiocarbon age calibration, 0–26 cal kyr BP. *Radiocarbon* 46:1029–1058.
- Reimer PJ, Baillie MGL, Bard E, Bayliss A, Beck JW, Blackwell PG, Bronk Ramsey C, Buck CE, Burr GS, Edwards RL, Friedrich M, Grootes PM, Guilderson TP, Hajdas I, Heaton T, Hogg AG, Hughen KA, Kaiser KF, Kromer B, McCormac FG, Manning SW, Reimer RW, Richards DA, Southon JR, Talamo S, Turney CSM, van der Plicht J, Weyhenmeyer CE. 2009. IntCal09 and Marine09 radiocarbon age calibration curves, 0–50,000 years cal BP. *Radiocarbon* 51:1111–1150.
- Reimer PJ, Bard E, Bayliss A, Beck JW, Blackwell PG, Bronk Ramsey C, Buck C, Cheng H, Edwards RL, Friedrich M, Grootes PM, Guilderson TP, Hafliðason H, Hajdas I, Hatté C, Heaton TJ, Hoffmann DL, Hogg AG, Hughen KA, Kaiser KF, Kromer B, Manning SW, Niu M, Reimer RW, Richards DA, Scott

- EM, Southon JR, Staff RA, Turney CSM, van der Plicht J. 2013. IntCal13 and Marine13 radiocarbon age calibration curves 0–50,000 years cal BP. *Radiocarbon* 55:1869–1887.
- Reimer PJ, Austin WEN, Bard E, Bayliss A, Blackwell P, Bronk Ramsey C, Butzin M, Edwards L, Friedrich M, Grootes PM, et al. 2020. The IntCal20 Northern Hemisphere radiocarbon calibration curve (0–55 cal kBP). *Radiocarbon* 62. This issue. doi: [10.1017/RDC.2020.41](https://doi.org/10.1017/RDC.2020.41).
- Rind D, Peteet D, Broecker W, McIntyre A, Ruddiman W. 1986. The impact of cold North Atlantic sea surface temperatures on climate: Implications for the Younger Dryas cooling (11–10 k). *Climate Dynamics* 1:3–33. doi: [10.1007/BF01277044](https://doi.org/10.1007/BF01277044).
- Southon J, Noronha AL, Cheng H, Edwards R, Wang Y. 2012. A high-resolution record of atmospheric ¹⁴C based on Hulu Cave speleothem H82. *Quaternary Science Reviews* 33:32–41. doi: [10.1016/j.quascirev.2011.11.022](https://doi.org/10.1016/j.quascirev.2011.11.022).
- Stuiver M, Polach HA. 1977. Discussion: Reporting of ¹⁴C data. *Radiocarbon* 19:355–363.
- Turney C, Fifield LK, Hogg A, Palmer J, Hughen K, Baillie M, Galbraith R, Ogden J, Lorrey A, Tims S, Jones R. 2010. Using New Zealand kauri (*Agathis australis*) to test synchronicity of abrupt climate change during the last glacial interval (60,000 to 11,000 years ago). *Quaternary Science Reviews* 29:3677–3682.
- Wang YJ, Cheng H, Edwards RL, An ZS, Wu JY, Shen CC, Dorale JA. 2001. A high-resolution absolute-dated Late Pleistocene monsoon record from Hulu Cave, China. *Science* 294:2345–2348.
- Yurco LN. 2010. A multi-proxy investigation of the late glacial “Mystery Interval” (17.5–14.5 ka) in the Cariaco Basin, Venezuela. Open access Theses 26. University of Miami. https://scholarlyrepository.miami.edu/oa_theses/26.